Copy
RM E57H09

NACA RM E57H09

NACA

RESEARCH MEMORANDUM

HEAT-EXCHANGER-CORE WEIGHTS FOR USE WITH HYDROGEN-EXPANSION TURBINE

By Thaine W. Reynolds

Lewis Flight Propulsion Laboratory
Cleveland, Ohio

Declassified by authority of NASA
Classification Notices No. 215

FACILITY FORM 602

N71-75112 (ACCESSION NUMBER) (THRU)
47 (PAGES) None (CODE)
/ (NASA CR OR TMX OR AD NUMBER) (CATEGORY)

NATIONAL ADVISORY COMMITTEE
FOR AERONAUTICS
WASHINGTON

CLASSIFIED

NATIONAL ADVISORY COMMITTEE FOR AERONAUTICS

RESEARCH MEMORANDUM

HEAT-EXCHANGER-CORE WEIGHTS FOR USE WITH HYDROGEN-EXPANSION TURBINE*

By Thaine W. Reynolds

SUMMARY

An analysis of probable heat-exchanger weights for stationary and rotary regenerator heat exchangers for use in a hydrogen-expansion turbine engine is presented. Heat-exchanger-core weights alone will probably be above 48 pounds per pound of hydrogen flow per second for stationary regenerators at a turbine-inlet temperature of 2000° R. This weight is for a pressure drop through the exchanger of about 10 percent of the inlet pressure.

Lowering the turbine-inlet temperature to about 1500° R would cut the regenerator-core weight in half.

Rotary regenerators offer possibilities for a considerably lighter heat-exchanger core, possibly one-fourth that of the stationary regenerators. At the same time, lower combustor temperatures may be employed. The mechanical problems associated with this type of exchanger may be quite severe.

Calculated physical properties of rich-mixture combustion products of hydrogen and air, which are required for heat-transfer calculations, are presented.

INTRODUCTION

One engine cycle that has been considered for possible high-speed, high-altitude aircraft use (ref. 1) is illustrated by the engine cross section shown in figure 1. In this cycle, which is called Rex III in reference 1, the cruise engine is essentially a ramjet burning hydrogen fuel. In order to obtain takeoff and boost thrust, a fan is provided at the inlet. The power to drive the fan is obtained by expanding hot hydrogen gas through the turbine. The hydrogen is heated in turn in a heat exchanger by the combustion products of the hydrogen with a portion of the total engine airflow.

An evaluation of the usefulness of this engine cycle will depend in part upon an analysis of the component weights. While it is realized that many of these component weights are interdependent, this report examines only the effect of varying parameters on the required heat-transfer area and probable weight of the heat-exchanger core itself. Heat exchangers of both the stationary and rotary type are considered.

In the particular cycle considered herein, the high-temperature combustion products for heating the hydrogen are obtained by burning hydrogen rich. The effect of obtaining the high temperatures by rich-mixture combustion rather than by lean is twofold: (1) The inner combustor is smaller, since much less air is required, and (2) the physical properties of the combustion gases are such that higher heat-transfer coefficients can be obtained, which would result in a smaller heat exchanger.

Mechanical problems associated with the design of these heat exchangers are not evaluated; only the performance is considered from the heat-transfer point of view. Physical properties of hydrogen and of combustion products of hydrogen-rich air mixtures of interest in heat-transfer calculations are presented.

This report presents the results of the analysis as generalizations independent of the heat-exchanger configurations to the extent possible. The calculations of actual core weight and pressure drops, however, obviously require selection of actual configurations. The heat-exchanger cores considered were taken from reference 2.

PHYSICAL PROPERTIES

Heat-transfer coefficient data are usually presented as correlations involving the dimensionless groups, Nusselt, Stanton, Reynolds, and Prandtl numbers. Evaluation of these groups requires certain physical property data for the fluid involved. The physical properties of hydrogen and the combustion products of rich hydrogen-air mixtures required for the analysis of the heat exchangers presented herein are (1) viscosity, (2) thermal conductivity, (3) specific heat, (4) mean molecular weight, (5) combustion temperature, and (6) enthalpy.

All symbols are defined in appendix A, and the method of calculating the properties of the mixtures is presented in appendix B. The calculated values are presented in figures 2 to 8.

ENGINE CYCLE

A diagram showing the components of an engine and the conditions under consideration in the following discussion is shown in figure 9. A

fuel flow rate of 6 pounds per second was chosen as a basis for presenting the calculations. This flow rate might correspond to the takeoff fuel flow rate for a 67-inch-diameter engine designed for Mach 4 at 100,000 feet. The total engine airflow would be about 300 pounds per second and the afterburner temperature about 3600° R.

Liquid hydrogen is pumped to approximately 8-atmosphere pressure and is vaporized and heated to the desired turbine-inlet temperature T_{c_o} by the heat exchanger. The hydrogen gas is expanded through the turbine to $2\frac{1}{2}$ atmospheres and a corresponding lower temperature. The hydrogen then enters the combustor where it combines with air from a secondary fan at 700° R and at a combustor pressure of about 2.2 atmospheres to arrive at a flame temperature T_{h_i}. This hot combustion gas enters the other side of the heat exchanger and exits from the heat exchanger at T_{h_o}. This fuel-rich mixture then combines with the major portion of the air, and a combustion temperature of about 3600° R is achieved. The gases are discharged through a suitable exhaust nozzle.

STATIONARY HEAT EXCHANGER

The variables will be discussed without reference to specific heat-exchanger cores insofar as possible. Calculations will then be presented for certain specific cores.

The required heat-exchanger area is determined from the relation

$$q/t = UA\,\Delta T \qquad (1)$$

For a hydrogen flow rate of 6 pounds per second and a turbine-inlet temperature of 2000° R, the required heat-exchanger capacity q/t is about 150,000,000 Btu per hour. For a selected combustion temperature and heat-exchanger arrangement (i.e., counterflow, crossflow with one fluid mixed, etc.), the ΔT of equation (1) is established. It is then only necessary to evaluate the over-all coefficient U to determine the heat-transfer area (and, hence, approximate heat-exchanger-core weight) required.

Combustion Temperature

The combustion temperature is determined by the equivalence ratio and the inlet temperatures of the fuel and air. The fuel temperature entering the combustor is assumed to be 700° R less than the heat-exchanger-outlet temperature. This temperature difference corresponds to the work required of the turbine to drive the fans.

In the following calculations, a turbine-inlet temperature of 2000° R will be assumed. The effect of varying this temperature will be considered in the section entitled Turbine-Inlet Temperature. The combustion temperature must be above 2000° R for a finite heat-exchanger area. An increase in the combustion temperature will require more air to be burned (lower equivalence ratio) since this is a rich-fuel combustor. The combustor cross-sectional area must then be increased if the same flow Mach number is to be maintained. As the equivalence ratio varies, the heat capacity and molecular weight of the combustion products vary. Table I shows the variations of some of these factors as the combustion temperature is changed from 2300° to 2900° R, while the combustor-exit Mach number is held at 0.1.

Table I also shows the increased effective temperature gradient for heat transfer ΔT_{lm} as the combustion temperature is increased. The ΔT_{lm} is the effective temperature gradient for counterflow arrangement. The relative heat-transfer area required would be decreased correspondingly as the combustion temperature is increased if the over-all transfer coefficient was not affected.

Relative combustor cross-sectional area and relative effective temperature gradient for heat transfer ΔT_{lm} for varying combustion temperatures are plotted in figure 10. For simplicity, this comparison is made by assuming counterflow arrangement. With a crossflow exchanger, a greater change in effective ΔT with changing combustion temperature would result.

Figure 10 shows that, unless the over-all heat-transfer coefficient decreases greatly as the combustion temperature increases, the smallest heat-exchanger area will be obtained by going to the highest combustion temperature compatible with structural limitations on the metal.

Heat-Transfer Coefficients

The final variable remaining to be determined in order to establish the heat-transfer area requirement is the over-all heat-transfer coefficient U. For negligible wall resistance, U is related to the individual coefficients by

$$U = \frac{1}{\frac{1}{h_c} + \frac{1}{h_h}} \tag{2}$$

Next to be examined are the probable values of the coefficients h_c and h_h and their variation with temperature.

The heat-transfer coefficient may be written as follows, from the definition of the Stanton number:

$$h = (St)C_p\rho V \tag{3}$$

By using the ideal equation of state $\rho = pm/RT$ and the relation for the speed of sound $V = M\sqrt{g\gamma RT/m}$, the above equation may be transformed to

$$h = (St)\frac{C_pM}{\sqrt{T}}\,p\sqrt{\frac{\gamma gm}{R}} \tag{4}$$

Experimental heat-transfer coefficients on the heat-exchanger cores to be compared later are plotted as $(St)(Pr)^{2/3}$ against Re. Equation (4) could be written

$$h = \frac{(St)(Pr)^{2/3}}{(Pr)^{2/3}}\,\frac{C_pM}{\sqrt{T}}\,p\sqrt{\frac{\gamma gm}{R}} \tag{5}$$

where p and T in this equation are static pressure and static temperature, respectively. The Mach number range is low enough that static and total temperature are considered the same. Static pressure is used throughout the comparison.

The probable range of heat-transfer coefficients for the fuel and combustion products can be estimated from equation (5).

Hydrogen. - For a constant pressure of 8 atmospheres and an assumed value of $(St)(Pr)^{2/3}$ of 0.003, the heat-transfer coefficient of the hydrogen will have the following variation with temperature and Mach number:

T, °R	C_p	Pr	h, Btu/(hr)(sq ft)(°F)
600	3.46	0.68	8060 M
1300	3.55	.685	5600 M
2000	3.69	.69	4680 M

This assumed value of $(St)(Pr)^{2/3}$ is in the range to be expected for flow of the hydrogen inside small tubes, which is the situation considered herein. Probable minimum values of the hydrogen-side coefficient are shown in figure 11.

It appears that, at the highest fuel temperature, if the flow Mach number is maintained above about 0.11, the heat-transfer coefficient should be at least 500 Btu/(hr)(sq ft)(°F).

Combustion products. - For a constant pressure of 2.2 atmospheres and an assumed value of $(St)(Pr)^{2/3} = 0.003$, the heat-transfer coefficient of the combustion products will vary with temperature and Mach number as follows:

T_{h_i}, °R	m	C_p	h, Btu/(hr)(sq ft)(°R)	Ratio, $h/h_{2900^\circ R}$
2300	7.45	1.06	811 M	1.38
2400	8.07	1.00	772 M	1.32
2500	8.7	.92	730 M	1.25
2700	10.17	.80	651 M	1.11
2900	11.46	.72	585 M	1.0

Probable minimum values of the hot-side coefficient are plotted in figure 12.

Thus, by maintaining the Mach number above 0.17, the minimum heat-transfer coefficient to be expected on the hot side should be at least 100 Btu/(hr)(sq ft)(°F), since the value of $(St)(Pr)^{2/3} = 0.003$ is near the minimum that will be encountered under the conditions considered. For flow over tubes of small diameter (as on the shell side of shell-tube exchangers), the value of $(St)(Pr)^{2/3}$ should be considerably higher than 0.003, and, hence, values of h of 100 or above may be obtained at considerably lower Mach numbers.

The last column in the previous table also shows how the heat-transfer coefficient of the combustion products varies as the temperature varies for a constant Mach number flow. The value at 2900° R is taken as the reference point. These relative values are plotted in figure 13 as a function of temperature along with the relative ΔT values from figure 10.

The heat-transfer coefficient of the combustion products, which should essentially control the over-all coefficient U, does not decrease as rapidly as the effective ΔT increases with increasing combustion temperature. Thus, it is apparent that the highest combustion temperature compatible with allowable metal wall temperatures will give the lower weight heat-exchanger cores.

Limiting Metal Temperature

The maximum equilibrium metal wall temperature will be determined by the maximum hot- and cold-gas temperatures and the ratio of the hot- to the cold-side heat-transfer coefficients:

$$T_w = \left(\frac{1}{1 + \frac{h_c}{h_h}}\right) T_{h_i} + \left(\frac{\frac{h_c}{h_h}}{1 + \frac{h_c}{h_h}}\right) T_{c_o} \qquad (6)$$

where the turbine-inlet temperature T_{c_o} is 2000° R.

The variation of metal temperature T_w with combustion temperature T_{h_i} is shown for several ratios of heat-transfer coefficients in figure 14(a).

For an estimate of maximum possible allowable metal temperatures with present materials, a plot of yield strength and 1000-hour rupture stress against temperature is shown (fig. 14(b)) for a high-temperature alloy, Inconel X (ref. 3). Depending upon the stress limitations of the design, it appears that metal temperatures of 2100° to 2200° R might be allowed, which would permit combustion temperatures close to 3000° R.

A 1/4-inch-diameter tube, for example, at 8-atmosphere (120 lb/sq in.) pressure and with a wall thickness of 0.012 inch would have a hoop stress in the wall of about 1190 pounds per square inch. At 2200° R, the indicated 1000-hour rupture stress (fig. 14(b)) for Inconel X is about 2500 pounds per square inch.

Turbine-Inlet Temperature

Decreasing the turbine-inlet temperature lowers the heat-exchanger capacity required and gives higher temperature differences for heat transfer for the same combustion temperature. Both of these factors decrease the heat-exchanger size. At the same time, however, a lower fuel temperature into the combustor results, and the burning of more air is required to reach the same combustion temperature. Thus, the combustor would be larger. Alternatively, the combustion temperature may be reduced.

Table II shows changes in pertinent variables as the turbine-inlet temperature is changed while the combustion temperature is held constant at 2900°, 2700°, and 2500° R.

The relative UA requirements for a given turbine-inlet temperature and combustion temperature are shown in the last column of table II. Counterflow arrangement is assumed for simplicity of analysis. The UA requirement for a turbine-inlet temperature of 2000° R and a combustion temperature of 2900° R is used as the basis for comparison. If the overall coefficient U is assumed to vary with combustion temperature as the heat-transfer coefficient of the combustion products, h_h curve in figure 13,

the relative heat-transfer-area change may be estimated by properly combining the h_h curve of figure 13 with the UA values of table II. This comparison is shown in figure 15.

From the curves of figure 15, it is apparent that decreasing the turbine-inlet temperature from 2000° to 1400° R would about cut the heat-exchanger weight in half at the combustion temperature level of 2900° R. Also, at the lower turbine-inlet temperature, the combustion temperature could be reduced several hundred degrees without greatly affecting the heat-exchanger area. At these lower turbine-inlet temperatures, the change in h_h nearly counteracts the change in effective ΔT, so that it would be more advantageous to go to the lower combustion temperatures.

Specific Heat-Exchanger Cores

The principal objective here was to establish a range of heat-transfer areas (and, hence, probable core weights) for a range of combustion-products-side pressure drops through the system. Since the weight was of primary concern, the minimum heat-transfer area for any allowable pressure drop was desired. For this reason, the various types of heat-exchanger cores in reference 2 were examined.

Previous discussion has pointed out that the heat-transfer coefficient on the hydrogen side of the exchanger should be easily maintained considerably higher than that expected on the combustion-products side. Further, the pressure drop on the hydrogen side could be increased, if necessary, by merely increasing the liquid pump discharge pressure. In calculating an over-all coefficient for heat transfer, the cold-side (hydrogen) coefficient was assumed equal to 500 Btu/(hr)(sq ft)(°F).

Heat exchangers of the shell-tube type, with the combustion products over the shell side, gave minimum heat-transfer-area requirements. In order to keep the pressure drop through the shell side of this exchanger in the neighborhood of 10 percent, the frontal area requirements are large, and the exchanger becomes voluminous. Without considering the practicality of such arrangements for this application, calculations are shown in table III for various cores and several inlet Mach numbers since the calculations yielded the minimum exchanger weights. The number identifying the core corresponds to the figure number of the performance curves in reference 2. The pressure drops were estimated by the method of reference 4.

The heat-transfer-area - pressure-drop relations from this table are plotted in figure 16. A curve bounding these points was drawn which essentially establishes a minimum heat-transfer area for a given pressure drop through the system. For a $\Delta p/p$ of 10 percent, a minimum heat-transfer area would appear to be about 570 square feet. If this core were made from 0.012-inch-thick stainless steel or Inconel, it would weigh about 1/2 pound per square foot, or about 285 pounds. This is approximately 48 pounds per pound of hydrogen flow per second.

[redacted]

ROTARY HEAT EXCHANGER

A schematic diagram of a rotary-heat-exchanger installation is shown in figure 17. The purpose of the rotary heat exchanger is exactly the same as for the stationary one. A rotary heat exchanger consists of a matrix of material which rotates and causes the matrix to pass alternately through the hot and cold fluids. Heat is thus transferred from the hot gas to the matrix, thence to the cold gas.

An additional variable to be chosen with the rotary exchanger is the capacity rate ratio C_r/C_{min}; that is, the ratio of the capacity rate of the core to the minimum capacity rate of the two gas flows. A smaller capacity rate ratio gives a greater temperature excursion to the matrix material, a resultant lower effective ΔT for heat transfer, and, hence, a greater area requirement and greater core weight. The rotative speed is lower for lower ratios of C_r/C_{min}.

A summary of design theory for rotary regnerators is given in reference 5, and effectiveness - NTU curves are given in reference 2. Experimental heat-transfer and friction drop performance for several wire-screen matrices is also given in reference 2. Data on these same matrices are extended to high Reynolds numbers in reference 6.

Since the core heat-transfer and flow areas are common to both heat-transfer fluids, the independent choice of flow conditions is more limited than with the stationary heat exchanger. In the case considered here, the hydrogen flow is considerably smaller than the combustion gas flow. One compromise that has to be made is to keep the hydrogen-side Mach number as low as possible to increase the flow area on that side without decreasing the heat-transfer coefficient of the hydrogen to too low a value.

Heat-Transfer Coefficients

The wire-screen matrices from reference 2 with the smallest wire diameters were used to establish the ranges of heat-transfer coefficients to be expected. Table IV lists some of the parameters of the matrices of interest. Again the number identifying the matrix corresponds to the figure number of the performance curve in reference 2 for that particular matrix. Small wire diameters which result in high heat-transfer coefficients and large heat-transfer areas per unit weight of core are the distinctive features of these matrices.

Hydrogen. - The heat-transfer coefficients for the hydrogen at two exit conditions, an exit hydrogen velocity of 200 feet per second ($M \equiv 0.024$) and 125 feet per second ($M \equiv 0.015$) and a temperature of 2000° R, are shown in table V.

The hydrogen experiences a large temperature change through the heat exchanger, and, hence, a considerable Reynolds number change because of the change in viscosity with temperature. The viscosity of hydrogen in this temperature range is proportional to $T^{0.695}$. Heat capacity and Prandtl number are essentially constant over this temperature range. The (St)(Pr) for these screen matrices was assumed to vary inversely with Reynolds number to $T^{0.375}$ (ref. 6), although this variation is slightly different than indicated on the curves of reference 2. Therefore, the heat-transfer coefficient will vary approximately directly with $T^{0.26}$.

A mean value of h_c was taken to be that at an average temperature of the hydrogen of about 1000° R. These estimated mean heat-transfer coefficients are also shown in table V.

Combustion products. - The range of heat-transfer coefficients for the combustion products at inlet conditions of 2300°, 2400°, and 2500° R and at inlet Mach numbers, based on free-flow area, of 0.04 and 0.06 are shown in table VI.

The viscosity of the combustion products varies directly as $T^{0.71}$, so that the heat-transfer coefficient varies about at $T^{0.27}$. A mean value of h_h was taken to be the value at the mean temperature of the combustion products. These estimated mean values are also shown in table VI.

Combustion Temperature

Some parts of the matrix material will approach the combustion temperature, so that the maximum allowable combustion temperature would be lower for the rotary than for the stationary heat exchanger.

To evaluate the heat-transfer-area requirements at various combustion temperatures, the following relations are used (ref. 5):

$$(NTU)_o = (NTU)_c \left[\frac{1}{1 + (hA)^*}\right] \tag{7}$$

$$(NTU)_c = \left(\frac{hA}{C}\right)_c \tag{8}$$

$$(hA)^* = \frac{(hA)_c}{(hA)_h} \tag{9}$$

At the flow velocities assumed in estimating the heat-transfer coefficients, the flow frontal areas are established. The ratio of heat-transfer areas A_c/A_h will be the same as the ratio of the flow frontal areas. Thus,

$$\frac{A_c}{A_h} = \left(\frac{w_c}{\rho_c V_c}\right)\left(\frac{\rho_h V_h}{w_h}\right) \tag{10}$$

The ratio of the heat-transfer coefficients h_c/h_h using the mean of values established previously is shown in table VI. The higher velocity flows of both sides are assumed together as one set of conditions and the lower velocity flows as another combination.

The variation of the flow parameters as combustion temperature varies is shown in table VII. In this table, the capacity rate ratio C_r/C_{min} was set at 2.0. The effect of a variation in this ratio will be discussed later.

From the values in tables V, VI, and VII and the core properties in table IV, the heat-transfer areas, core weights, and speeds can be calculated.

The calculations of heat-transfer area, core weight, and rotational speed for the three matrices at combustion temperatures of 2300°, 2400°, and 2500° R are shown in table VIII. These values are for a turbine-inlet temperature of 2000° R and a capacity rate ratio C_r/C_{min} of 2.0.

It will be noted, as with the stationary exchanger, that, as the combustion temperature is increased, the required heat-exchanger area and weight decrease. However, the required rotational speed is increased as the weight is decreased, since the matrix core capacity rate C_r is constant.

The friction pressure drop for these configurations can be estimated from the relation

$$\frac{\Delta p}{p} = f\left(\frac{A}{A_f}\right)\frac{\gamma}{2}M^2 \tag{11}$$

This relation is derived from the usual Fanning equation:

$$\Delta p = 4f\,\frac{L}{D_h}\,\frac{\rho V^2}{2g}$$

By substituting,

$$\frac{4L}{D_h} = \frac{A}{A_f}$$

and

$$\frac{\rho V^2}{2g} = \frac{\gamma}{2}pM^2$$

Pressure drops so calculated are also shown in table VIII for the combustion-products side of the exchanger. The core weight and pressure drop relation are shown in figure 18.

A comparison of some of the core weights and corresponding pressure drops in figure 18 with those for the stationary exchangers (fig. 16) shows the marked reduction in heat-exchanger-core weight possible with the rotary exchanger.

For core number 108 at a combustion temperature of 2500° R, the core weight would appear to be about 70 pounds at a pressure drop of 10 percent. This weight is only about one-fourth the minimum estimated for the stationary-exchanger core for the same pressure drop. Furthermore, the combustion temperature is 400° R lower for the rotary exchanger in this comparison.

It should again be pointed out here that no evaluation of the mechanical problems associated with the rotary exchanger is included herein. It is recognized that the additional structural complexity required for the rotary exchanger might modify these weight comparisons.

Capacity Rate Ratio

From the curves of temperature effectiveness against the number of transfer units $(NTU)_o$ (ref. 2), it can be seen that increasing the capacity rate ratio will decrease the $(NTU)_o$ for the same effectiveness. The core weight required will decrease in direct proportion to this change in $(NTU)_o$. However, when the capacity rate of the matrix is increased, the speed must be increased since it is the product of (weight)×(speed)×(metal heat capacity), which comprises the matrix capacity rate.

A change in the capacity rate ratio also changes the temperature excursion which the core metal takes. The range of temperature through which the metal passes is

$$(\Delta T)_{metal} = \frac{q/t}{(\text{core weight})\times(\text{rpm}\times 60)\times(C_{p_{metal}})} \qquad (12)$$

so that the ΔT of the metal is inversely proportional to the capacity rate ratio for a given rate of heat exchange.

Turbine-Inlet Temperature

As with the stationary heat exchanger, lowering the turbine-inlet temperature decreases the rate of heat exchange and increases the effective

temperature difference for heat transfer. Both factors tend to decrease the heat-exchanger-core weight.

However, if the capacity rate ratio C_r/C_{min} is held constant, the speed of rotation is increased. Since C_{min} is not a function of the quantity of heat exchanged, C_r is not changed. Hence, since core weight times speed is constant, the speed must vary inversely with the weight change.

The estimated change in heat-exchanger-core weight with changing turbine-inlet temperature is shown in figure 19 for a combustion temperature of 2500° R. It appears that the core weight could be reduced by one-half by lowering the turbine-inlet temperature to about 1500° R. This is about the same ratio as was estimated for the stationary exchanger also.

Lowering the turbine-inlet temperature will also decrease the variation in the core metal temperature, since the temperature excursion of the metal is changed in direct proportion to the rate of heat exchanged.

CONCLUSIONS

Through an analysis of the heat-transfer performance possibilities of stationary and rotary heat exchangers for use in a hydrogen-expansion turbine engine, a system called Rex III in reference 1, the following conclusions have been drawn:

1. For stationary heat exchangers, core weights alone would be above 48 pounds per pound per second of hydrogen flow at a turbine-inlet temperature of 2000° R and for a pressure drop of about 10 percent of the inlet combustion gas pressure.

2. Rotary regenerators offer possibilities for heat-exchanger-core weights one-fourth that of the stationary exchanger for the same pressure drop. At the same time, lower combustion temperatures may be used.

3. Lowering the turbine-inlet temperature to about 1500° R would cut the heat-exchanger-core weight about in half for either type of exchanger.

CONCLUDING REMARKS

While the analysis shows that the heat-exchanger-core weight for a rotary heat exchanger may be considerably smaller than that for a stationary exchanger to do the same job, it should be kept in mind that the mechanical problems with the rotary exchanger may be quite severe.

In particular, at the present state of the art, the seals necessary to prevent too high a hydrogen leakage at the high differential pressures involved are a formidable problem. A high rate of hydrogen leakage would reduce the quantity of turbine working fluid and would affect the heat-exchanger performance adversely. The high temperature levels and temperature changes in the system will cause thermal expansion problems that will aggravate the sealing problem.

Contamination of the hydrogen by carryover of combustion products trapped in the matrix is small, less than 1/2 percent for the conditions considered herein, so that the effect on the physical properties of the hydrogen would be negligible.

The analysis presented herein compares only weights of the heat-exchanger cores based on their heat-transfer performance. The additional mechanical complexity of the rotary exchanger may add more to its weight than that of a stationary exchanger. The amount cannot be estimated until some satisfactory seal designs are developed to operate at these conditions.

Lewis Flight Propulsion Laboratory
National Advisory Committee for Aeronautics
Cleveland, Ohio, August 14, 1957

APPENDIX A

SYMBOLS

A	heat-transfer area, sq ft
A_f	free-flow frontal area, sq ft
A_{ij}	function, defined in text
C	capacity ratio, wC_p, Btu/(hr)($^\circ$R)
C_p	heat capacity at constant pressure, Btu/(lb)($^\circ$R)
C_r	core capacity ratio, (core weight)×(core heat capacity)×(rpm×60), Btu/(hr)($^\circ$R)
D	diameter, ft
f	friction factor
g	conversion factor, 32.174 ft/sec^2
H	enthalpy, Btu
h	heat-transfer film coefficient, Btu/(hr)(sq ft)($^\circ$R)
$(hA)^*$	$(hA)_c/(hA)_h$
k	thermal conductivity, Btu/(hr)(sq ft)($^\circ$F/ft)
L	flow length, ft
M	Mach number, $V/\sqrt{\gamma gRT/m}$
m	molecular weight
NTU	number of transfer units of an exchanger, AU/C_{min}
$(NTU)_o$	number of over-all transfer units of an exchanger
Pr	Prandtl number, $C_p\mu/k$
p	pressure, lb/sq ft
q	heat transferred, Btu

[redacted]

R	universal gas constant, 1544 ft-lb/(lb mole)(^{o}R)
Re	Reynolds number, $4r_h V\rho/\mu$
$4r_h$	hydraulic diameter, ft
S	Sutherland constant
St	Stanton number, $h/C_p\rho V$
T	temperature, ^{o}R
ΔT_{lm}	log mean temperature difference for heat transfer, $\dfrac{(T_{h_o} - T_{c_i}) - (T_{h_i} - T_{c_o})}{\ln_e \dfrac{T_{h_o} - T_{c_i}}{T_{h_i} - T_{c_o}}}$
t	time, hr
U	over-all heat transfer coefficient, Btu/(hr)(sq ft)(^{o}F)
V	velocity, ft/hr
w	weight-flow rate, lb/hr
x	mole fraction
γ	ratio of specific heats
ε	heat-transfer effectiveness, $\dfrac{C_h}{C_{min}}\left(\dfrac{T_{h_i} - T_{h_o}}{T_{h_i} - T_{c_i}}\right) = \dfrac{C_c}{C_{min}}\left(\dfrac{T_{c_o} - T_{c_i}}{T_{h_i} - T_{c_i}}\right)$
μ	viscosity, lb/(ft)(hr)
ρ	density, lb/cu ft
φ_{ij}	function, defined in text

Subscripts:

a	air
c	cold side

CLASSIFIED

c_i	cold gas in
c_o	cold gas out
f	fuel
h	hot side
h_i	hot gas in
h_o	hot gas out
i	component i
j	component j
m	mixture
min	minimum
w	wall

APPENDIX B

PHYSICAL PROPERTIES

The mixture compositions for which the physical properties are presented are those resulting from the reaction

$$n(2H_2) + O_2 + 3.77\ N_2 \rightarrow 2H_2O + 3.77\ N_2 + 2(n - 1)H_2$$

where n will vary from 1 (stoichiometric) to infinity (pure H_2). No dissociation is assumed at any condition encountered herein, since temperatures are below 3000° R.

The composition parameter used for the physical property plots is mole fraction of H_2 in the mixture of combustion products. At a hydrogen concentration of zero, the mole fraction of hydrogen is zero, and water and nitrogen are in the mole ratio 2.0 to 3.77. This is the composition resulting from stoichiometric combustion (n = 1). A mole fraction equal to 1 is pure hydrogen. An equivalence ratio scale is also included on the plots for reference. Equivalence ratio is the ratio of actual fuel to that required for stoichiometric combustion.

Experimental viscosity and thermal conductivity data are available for the pure component gases (ref. 7). Heat capacities for the pure gases were taken from reference 8. Properties of normal-hydrogen gas were used throughout, since all data were not available for the para-hydrogen. The difference in properties between normal and para-hydrogen would not affect appreciably any of the results presented herein.

Physical property data for the mixtures were calculated by the methods outlined as follows. Although, as is discussed in the references cited, these equations are not considered applicable when one of the gases is highly polar (water vapor in this instance), the relations were nevertheless assumed to apply, since no experimental data for these mixtures were available.

Viscosity

The viscosities of the mixtures were calculated according to the method of reference 9:

$$\mu_m = \sum_{i=1}^{n} \frac{\mu_i}{1 + \frac{1}{x_i} \sum_{\substack{j=1 \\ j \neq 1}}^{n} x_j \varphi_{ij}}$$

$$\varphi_{ij} = \frac{\left[1 + \left(\frac{\mu_i}{\mu_j}\right)^{1/2}\left(\frac{m_j}{m_i}\right)^{1/4}\right]^2}{\frac{4}{\sqrt{2}}\left(1 + \frac{m_i}{m_j}\right)^{1/2}}$$

Pure component gas viscosities were taken from reference 7. Values of φ_{ij} are plotted in reference 9 for simplifying the calculations. Calculated curves are shown in figure 2. For values at intermediate temperatures, the mean temperature dependence of viscosity is approximately $\mu \propto T^{0.71}$.

Thermal Conductivity

The thermal conductivities of the mixtures were calculated according to a similar expression (ref. 10):

$$k_m = \sum_{i=1}^{n} \frac{k_i}{1 + \frac{1}{x_i}\sum_{\substack{j=1 \\ j\neq i}}^{n} x_{ij} A_{ij}}$$

$$A_{ij} = \frac{1}{4}\left\{1 + \left[\frac{\mu_i}{\mu_j}\left(\frac{m_j}{m_i}\right)^{0.75}\frac{\left(1 + \frac{S_i}{T}\right)}{\left(1 + \frac{S_j}{T}\right)}\right]^{1/2}\right\}^2 \frac{1 + \frac{S_{ij}}{T}}{1 + \frac{S_i}{T}}$$

The pure component thermal conductivities were taken from reference 7.

The calculated gas-mixture thermal conductivities are shown in figure 3. For values at intermediate temperatures the temperature dependence of thermal conductivity is approximately $k \propto T^{0.77}$.

Heat Capacity

The heat capacities of the gas mixtures were taken as the mass average of the heat capacities of the constituents:

$$C_{p_m} = \sum x_i C_{p_i}$$

The pure component heat capacities were taken from reference 8. The calculated gas-mixture heat capacities are plotted in figure 4.

Flame Temperature

Rich-mixture flame temperatures were calculated for the reaction

$$n(2H_2) + O_2 + 3.77\ N_2 \rightarrow 2H_2O + 3.77\ N_2 + 2(n - 1)H_2$$

by assuming no dissociation of the products of combustion. The heat balance is

$$w_m \int_{T_a}^{T_f} C_{p_m}\, dT = (2)(2.016)(51{,}570) + 2n(2.016)(T_{H_2} - T_a)$$

where T_a, the entering air temperature, was set at 700° R and T_{H_2}, the entering hydrogen temperature, was set at values of 700°, 900°, 1100°, and 1300° R.

Curves of rich-mixture flame temperature against equivalence ratio are plotted in figure 5.

Other Calculated Values

The Prandtl number $C_p\mu/k$ was computed from the curves of figures 2, 3, and 4 and is shown in figure 6.

Mean molecular weights were taken as the volumetric average of the molecular weights of the constituents:

$$m_m = \sum x_i m_i$$

Values of the mean molecular weight for a range of equivalence ratios are plotted in figure 7.

The enthalpy of hydrogen from the normal liquid state to 2000° R is plotted in figure 8. Liquid hydrogen at 1 atmosphere is taken as the zero reference point.

REFERENCES

1. Rae, Randolph S.: Various Engine Cycles Using Hydrogen as a Working Fluid and as a Fuel. Paper presented at meeting Inst. Aero. Sci., Cleveland (Ohio), Mar. 14, 1957.

2. Kays, W. M., and London, A. L.: Compact Heat Exchangers. The Nat. Press, Palo Alto (Calif.), 1955.

3. Anon.: Inconel "X" - A High Strength, High Temperature Alloy. Dev. and Res. Div., The International Nickel Co., Inc., Jan. 1949.

4. Hubbartt, James E., Slone, Henry O., and Arne, Vernon L.: Method for Rapid Determination of Pressure Change for One-Dimensional Flow with Heat Transfer, Friction, Rotation, and Area Change. NACA TN 3150, 1954.

5. Coppage, J. E., and London, A. L.: The Periodic-Flow Regenerator - A Summary of Design Theory. Trans. ASME, vol. 75, no. 5, July 1953, pp. 779-787.

6. Tong, Long Sun: Heat Transfer and Friction Characteristics of Screen Matrices at High Reynolds Number. Tech. Rep. No. 28, Dept. Mech. Eng., Stanford Univ., Apr. 1956. (Contract N-onr-22523.)

7. Hilsenrath, Joseph, et al.: Tables of Thermal Properties of Gases. Circular 564, NBS, Nov. 1, 1955.

8. Hougen, O. A., and Watson, K. M.: Industrial Chemical Calculations. Second ed., John Wiley & Sons, Inc., 1936, p. 114.

9. Bromley, L. A., and Wilke, C. R.: Viscosity Behavior of Gases. Ind. and Eng. Chem., vol. 43, no. 7, July 1951, pp. 1641-1648.

10. Lindsay, Alexander L., and Bromley, LeRoy A.: Thermal Conductivity of Gas Mixtures. Ind. and Eng. Chem., vol. 42, no. 8, Aug. 1950, pp. 1508-1511.

TABLE I. - VARIATION OF FLOW PARAMETERS OF COMBUSTOR AND STATIONARY HEAT EXCHANGER WITH COMBUSTION TEMPERATURE

[Turbine-inlet temperature, 2000° R; combustor-exit Mach number, 0.1; heat-transfer rate, 150×10^6 Btu/hr.]

Combustion temperature, T_{h_i}, °R	Equivalence ratio	Mean molecular weight, m	Airflow rate, w_a, lb/sec	Total hot-gas flow, w_h, lb/sec	Heat capacity of combustion products, $C_{p,h}$, Btu/(lb)(°R)	Density of combustion products, ρ_{h_i}, lb/cu ft	Gas velocity at combustor exit (M=0.1), V	Combustor-exit area, sq ft	ΔT_h, °R	Heat-exchanger-exit temperature, T_{h_o}, °R	Log mean temperature difference for counterflow, ΔT_{lm}, °R	Relative UA required (counterflow)
2300	10.0	7.45	20.35	26.35	1.06	0.00978	450	6.00	1495	815	505	2.42
2400	8.7	8.07	23.4	29.4	1.00	.0101	442	6.59	1415	985	635	1.93
2500	7.7	8.7	26.4	32.4	.92	.0105	435	7.11	1400	1100	745	1.65
2700	6.1	10.17	33.3	39.3	.80	.0113	418	8.34	1325	1375	985	1.24
2900	5.0	11.46	40.4	46.4	.72	.0119	407	9.58	1240	1660	1225	[a]1.00

[a]Basis of comparison.

TABLE II. - VARIATION OF FLOW PARAMETERS OF COMBUSTOR AND STATIONARY HEAT EXCHANGER WITH VARYING TURBINE-INLET TEMPERATURE AND COMBUSTION TEMPERATURE

Combustion temperature, T_{h_i}, $^{\circ}R$	Turbine-inlet temperature, T_{c_o}, $^{\circ}R$	Fuel, ΔH, Btu/lb	Relative heat-exchange rate[a]	Equivalence ratio	Airflow rate, w_a, lb/sec	Total hot-side flow, w_h, lb/sec	Heat capacity of combustion products, $(\bar{C}_p)_h$, Btu/(lb)($^{\circ}R$)	Capacity rate of hot side, $(wC_p)_h$	ΔT_h, $^{\circ}R$	Heat-exchanger-exit temperature, T_{h_o}, $^{\circ}R$	Log mean temperature difference for counterflow, ΔT_{lm}, $^{\circ}R$	Relative UA required
2900	2000	6940	1.0	5.0	40.6	46.6	0.72	33.6	1240	1660	1225	[b]1.0
	1800	6200	.893	4.5	45.1	51.1	.70	35.8	1040	1860	1430	.765
	1600	5460	.786	4.1	49.6	54.6	.67	36.6	895	2005	1610	.599
	1400	4720	.68	3.7	55.0	61.0	.65	39.7	715	2185	1800	.463
2700	2000	6940	1.0	6.1	33.3	39.3	.80	31.4	1325	1375	985	1.24
	1800	6200	.893	5.4	37.7	43.7	.77	33.7	1105	1595	1200	.912
	1600	5460	.786	4.9	41.5	47.5	.72	34.2	960	1740	1380	.699
	1400	4720	.68	4.4	46.2	52.2	.70	36.6	775	1925	1575	.529
2500	2000	6940	1.0	7.7	26.4	32.4	.92	29.8	1400	1100	745	1.64
	1800	6200	.893	6.5	31.3	37.3	.84	31.3	1190	1310	955	1.146
	1600	5460	.786	5.8	35.1	41.1	.78	32.1	1020	1480	1150	.838
	1400	4720	.68	5.2	39.1	45.1	.75	33.8	840	1660	1345	.62

[a]Relative heat-exchange rate = $\Delta H_{fuel}/\Delta H_{fuel}$ at 2000° R.

[b]Basis for comparison.

TABLE III. - STATIONARY-EXCHANGER-CORE HEAT-TRANSFER AREAS AND PRESSURE RATIOS ACROSS HOT SIDE

[Turbine-inlet temperature, 2000° R; combustion temperature, 2900° R; shell side.]

Core number or figure number in ref. 2	Inlet Mach number (based on free-flow area)	Hydraulic diameter, $4r_h$, ft	Reynolds number, Re	$(St)(Pr)^{2/3}$	Friction factor, f	Heat-transfer coefficient, h_h, Btu/(hr)(sq ft)(°F)	Over-all heat-transfer coefficient, U	Heat-transfer area, A, sq/ft	Pressure-drop ratio, $\Delta p/p$
44	0.1	0.0166	2390	0.014	0.072	272	176	695	0.025
46	↓	.0125	1790	.012	.047	233	159	770	.015
47		.0196	2800	.013	.063	252	167	733	.022
52		.0166	2390	.011	.052	214	150	816	.022
44	.15	.0166	3590	.012	.069	348	205	597	.077
46	↓	.0125	2680	.010	.042	290	183	667	.058
47		.0196	4200	.0105	.06	305	189	646	.07
52		.0166	3590	.011	.057	320	195	627	.063
44	.20	.0166	4780	.011	.065	426	230	532	.157
46	↓	.0125	3580	.009	.04	349	205	597	.101
47		.0196	5600	.01	.058	387	219	559	.144
52		.0166	4780	.0098	.057	380	216	567	.144

TABLE IV. - PROPERTIES OF SOME ROTARY-HEAT-EXCHANGER MATRICES

Matrix number or figure number in ref. 2	Wire diameter, in.	Hydraulic diameter, $4r_h$, ft	Heat-transfer area per unit volume, $\frac{\text{sq ft}}{\text{cu ft}}$	Porosity	Bulk density, lb/cu ft	Weight per unit heat-transfer area, lb/sq ft
107	0.0105	0.001328	1820	0.602	198	0.11
108	.0076	.001292	2090	.675	$162\frac{1}{2}$	.0777
109	.0135	.002960	980	.725	$137\frac{1}{2}$	.1403

TABLE V. - HEAT-TRANSFER COEFFICIENTS FOR HYDROGEN IN ROTARY HEAT EXCHANGER

Matrix number or figure number in ref. 2	Exit velocity, ft/sec	Reynolds number, Re	(St)(Pr)	Friction factor, f	Heat-transfer coefficient, h, 2000° R	Heat-transfer coefficient, h, 1000° R
107	125	126	0.07	1.0	1850	1545
108		123	.072	.97	1905	1590
109		281	.063	.50	1668	1390
107	200	202	0.057	.85	2420	2020
108		196	.056	.80	2385	1990
109		450	.050	.42	2120	1770

TABLE VI. - HEAT-TRANSFER COEFFICIENTS FOR COMBUSTION PRODUCTS IN ROTARY HEAT EXCHANGER

Combustion temperature, T_{h_i}, °R	Matrix number or figure number in ref. 2	Reynolds number, Re	(St)(Pr)	Friction factor, f	Heat-transfer coefficient, $h_{T_{h_i}}$	Heat-transfer coefficient, h_h	Heat-transfer coefficient, h_c	Ratio of cold- to hot-side coefficient, h_c/h_h
Mach number, 0.04								
2300	107	90.5	0.078	1.2	1070	961	1545	1.61
	108	88	.081	1.1	1110	997	1590	1.60
	109	201	.072	.55	986	887	1390	1.57
2400	107	88.5	.079	1.25	1033	940	1545	1.64
	108	86	.081	1.1	1060	964	1590	1.65
	109	197	.072	.55	942	858	1390	1.62
2500	107	83.4	.079	1.3	960	878	1545	1.76
	108	80.7	.082	1.15	995	910	1590	1.75
	109	185	.075	.56	911	834	1390	1.67
Mach number, 0.06								
2300	107	135.5	0.069	1.0	1420	1275	2020	1.58
	108	132	.07	.91	1440	1292	1990	1.54
	109	302	.06	.48	1234	1110	1770	1.59
2400	107	132.8	.069	1.0	1360	1240	2020	1.63
	108	129	.07	.91	1380	1260	1990	1.58
	109	296	.061	.49	1200	1095	1770	1.62
2500	107	125	.07	1.1	1272	1165	2020	1.73
	108	121	.072	.98	1310	1200	1990	1.66
	109	278	.064	.50	1162	1065	1770	1.66

[redacted]

TABLE VII. - VARIATION OF FLOW PARAMETERS IN COMBUSTOR AND ROTARY HEAT EXCHANGER WITH COMBUSTION TEMPERATURE

[Turbine-inlet temperature, 2000° R; capacity rate ratio, C_r/C_{min}, 2.0.]

Combustion temperature, T_{h_i}, °R	Equivalence ratio	Hot-gas flow, w_h, lb/sec	Heat capacity of hot gas, $(C_p)_h$	Capacity rate of hot side, $(wC_p)_h$	Capacity rate ratio of gas flows, $\frac{C_{min}}{C_{max}}$	Heat-transfer effectiveness, ε	Over-all number of transfer units required, $(NTU)_o$	Heat-transfer-area ratio, A_c/A_h
2300	10.0	26.35	1.06	27.9	0.75	0.867	4.6	0.274
2400	8.7	29.4	1.00	29.4	.71	.83	3.5	.248
2500	7.7	32.4	.92	29.8	.70	.797	3.0	.226

TABLE VIII. - HEAT-TRANSFER AREAS, WEIGHTS, SPEEDS, AND PRESSURE DROPS

FOR ROTARY HEAT EXCHANGER AT VARIOUS COMBUSTION TEMPERATURES

Combustor-inlet temperature, T_{h_i}, °R	Matrix core number or figure number of ref. 2	$(NTU)_o$	(hA)*	$(NTU)_c$	Cold-side heat-transfer area, sq ft	Total heat-transfer area, sq ft	Core weight, lb	Core rotational speed, rpm	Friction-factor hot side, f	Pressure drop ratio on hot side, $(\Delta p/p)_h$
Hydrogen exit Mach number, 0.015; combustion-products inlet Mach number, 0.04 (based on free-flow areas)										
2300	107	4.6	0.441	6.53	319	1485	163	129	1.2	0.097
	108		.439	6.61	314	1460	114	184	1.1	.086
	109		.430	6.57	358	1665	234	90	.55	.049
2400	107	3.5	0.406	4.92	241	1212	133	158	1.25	0.075
	108		.409	4.93	235	1182	92	228	1.1	.064
	109		.401	4.91	267	1343	189	111	.55	.036
2500	107	3.0	0.398	4.19	205	1110	122	172	1.3	0.067
	108		.396	4.19	199	1080	84	250	1.15	.057
	109		.378	4.13	225	1220	171	123	.56	.031
Hydrogen exit Mach number, 0.024; combustion-products inlet Mach number, 0.06										
2300	107	4.6	0.433	6.59	247	1150	126	167	1.0	0.223
	108		.422	6.54	248	1152	90	234	.91	.204
	109		.435	6.60	282	1310	184	114	.48	.122
2400	107	3.5	0.404	4.91	184	924	101	208	1.0	0.165
	108		.392	4.87	185	929	72	292	.91	.152
	109		.401	4.90	209	1050	147	143	.49	.092
2500	107	3.0	0.391	4.17	156	845	93	226	1.1	0.154
	108		.375	4.12	157	846	66	318	.96	.136
	109		.375	4.12	176	953	134	152	.50	.079

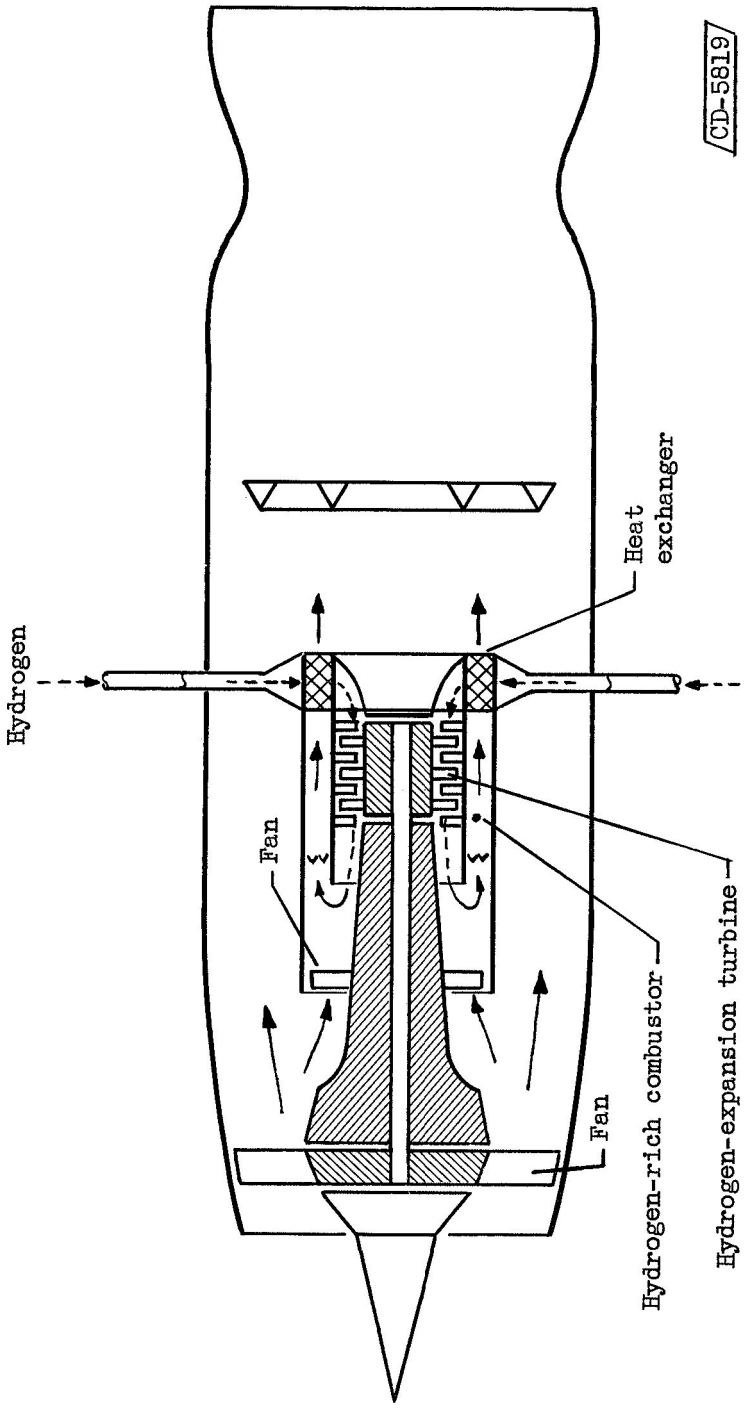

Figure 1. - Schematic cross-sectional diagram of hydrogen-expansion engine.

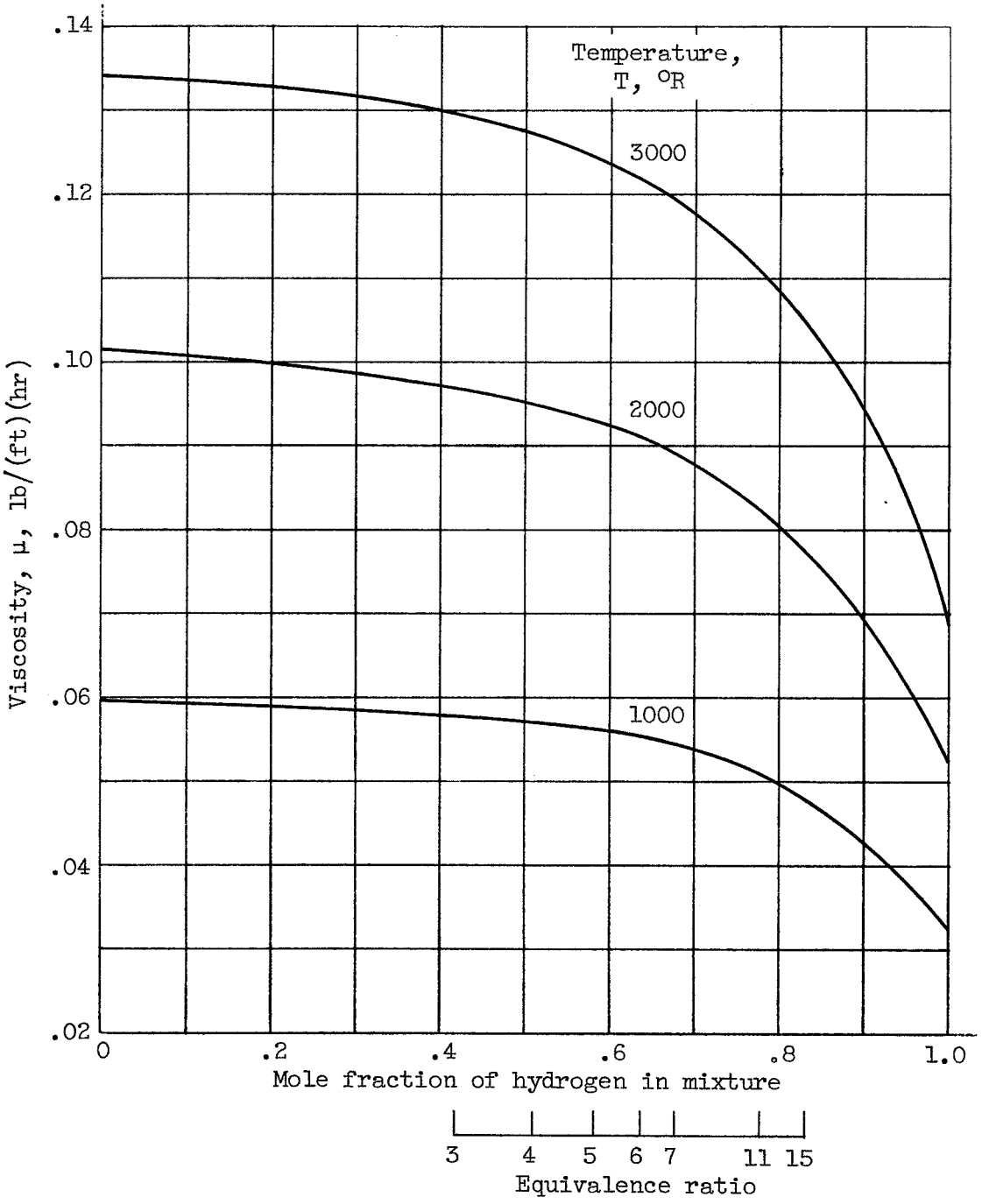

Figure 2. - Calculated viscosity of hydrogen-nitrogen-water vapor mixtures. Mole ratio of nitrogen/water = 3.77/2.0; $\mu \propto T^{0.71}$.

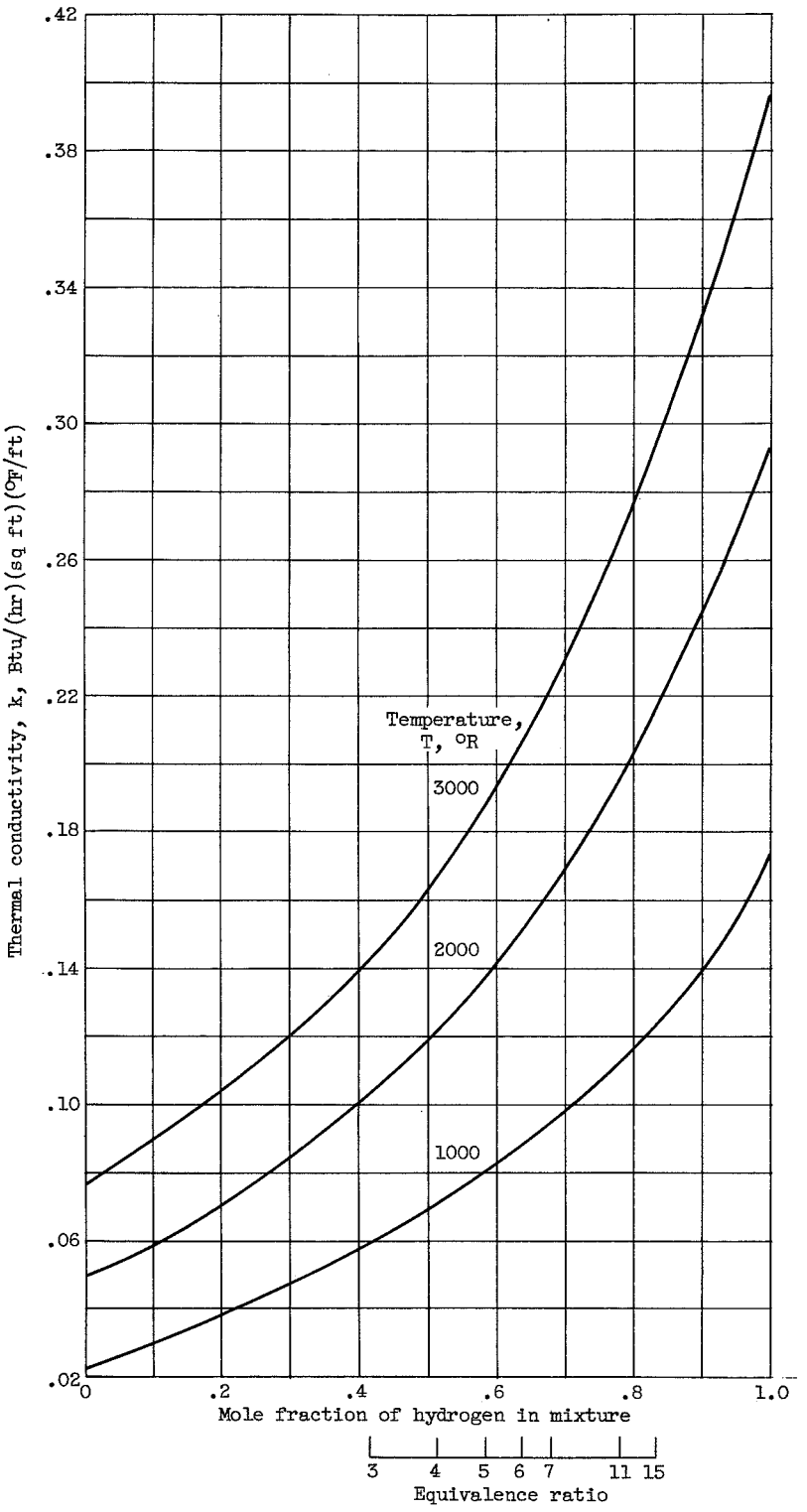

Figure 3. - Calculated thermal conductivity of hydrogen-nitrogen-water vapor mixtures. Mole ratio of nitrogen/water = 3.77/2.0; $k \propto T^{0.77}$.

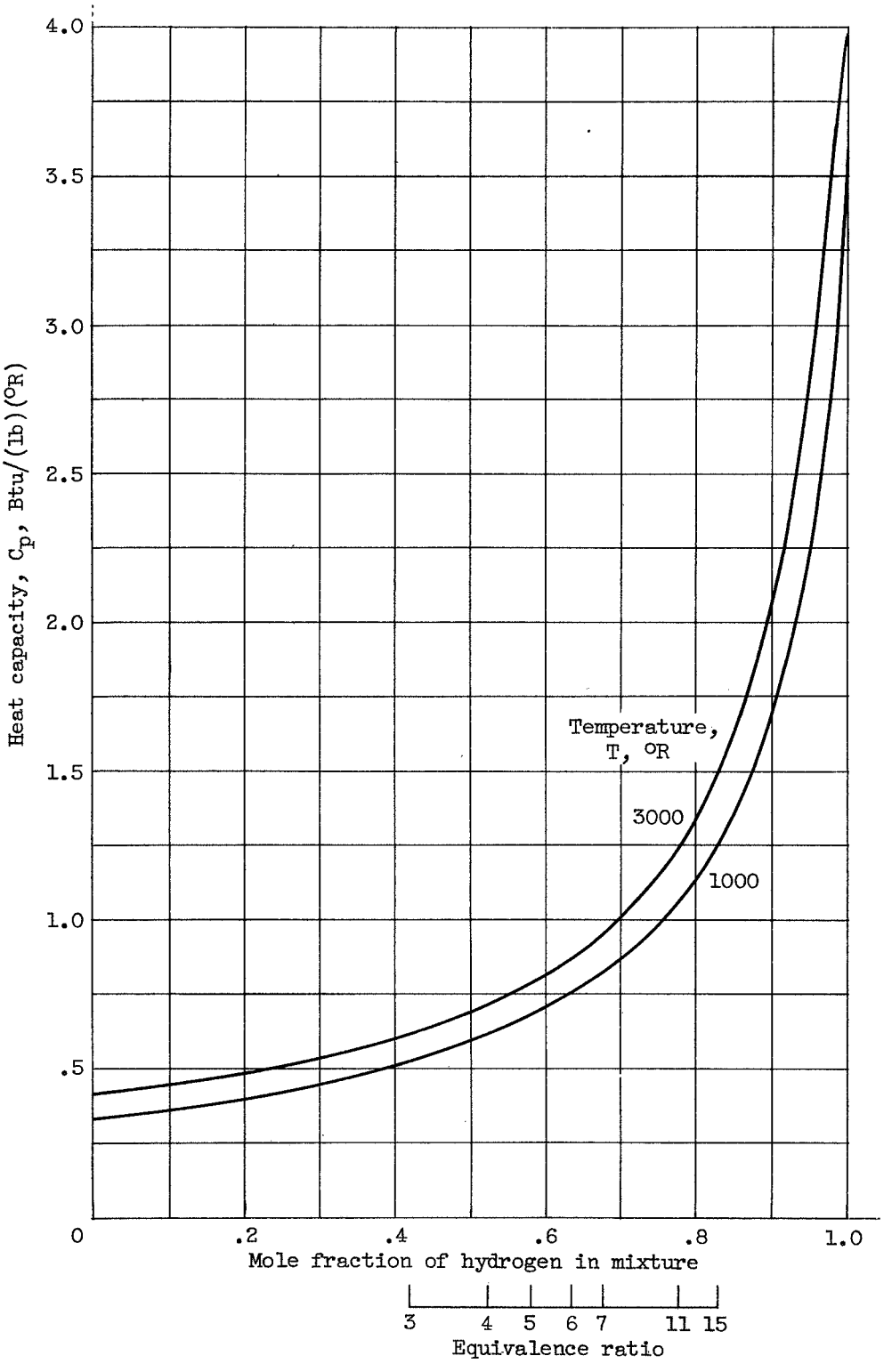

Figure 4. - Heat capacity of hydrogen-nitrogen-water vapor mixtures. Mole ratio of nitrogen/water = 3.77/2.0.

4558

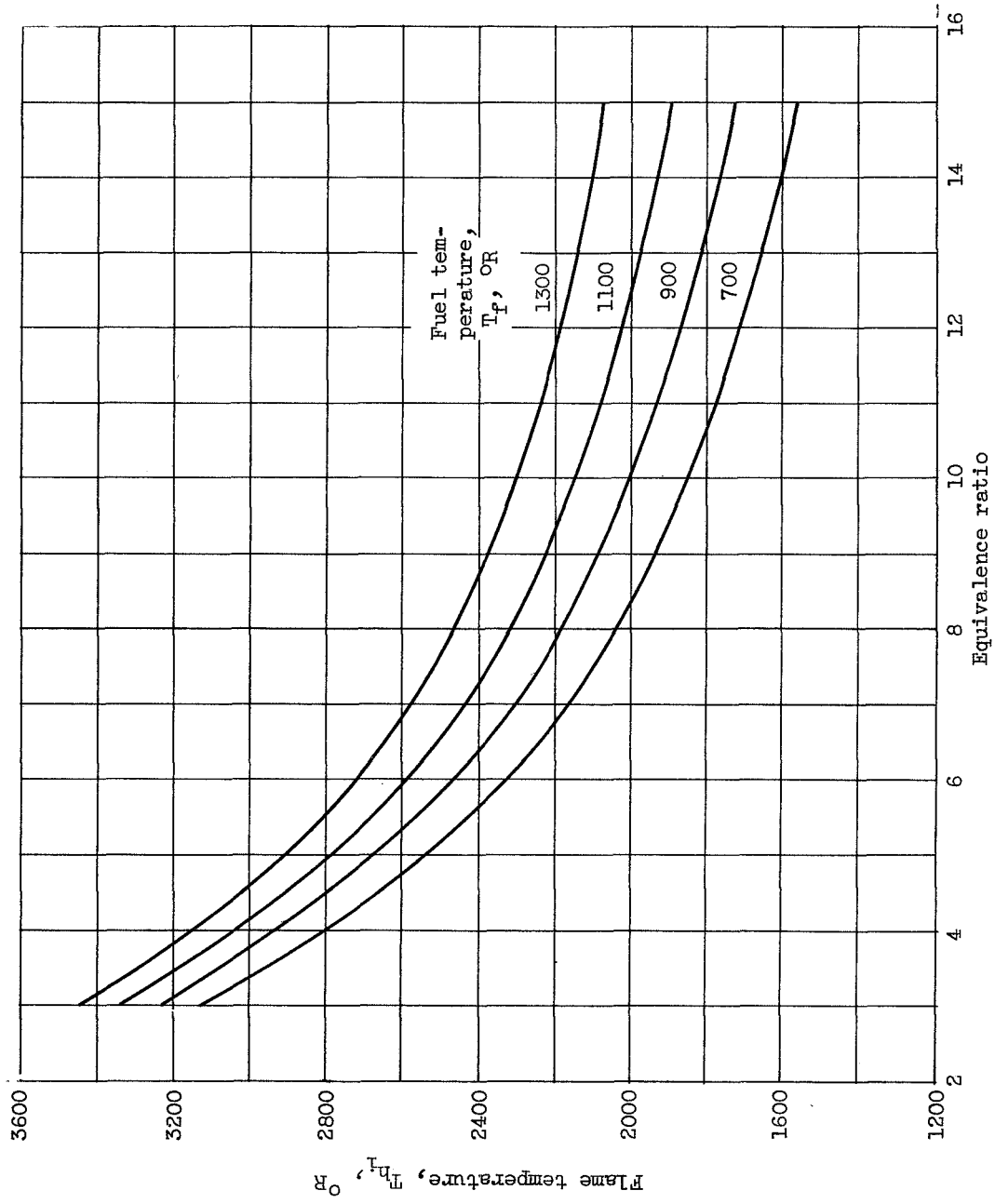

Figure 5. - Calculated rich-mixture flame temperatures for hydrogen-air mixtures. No dissociation assumed; air temperature, 700° R.

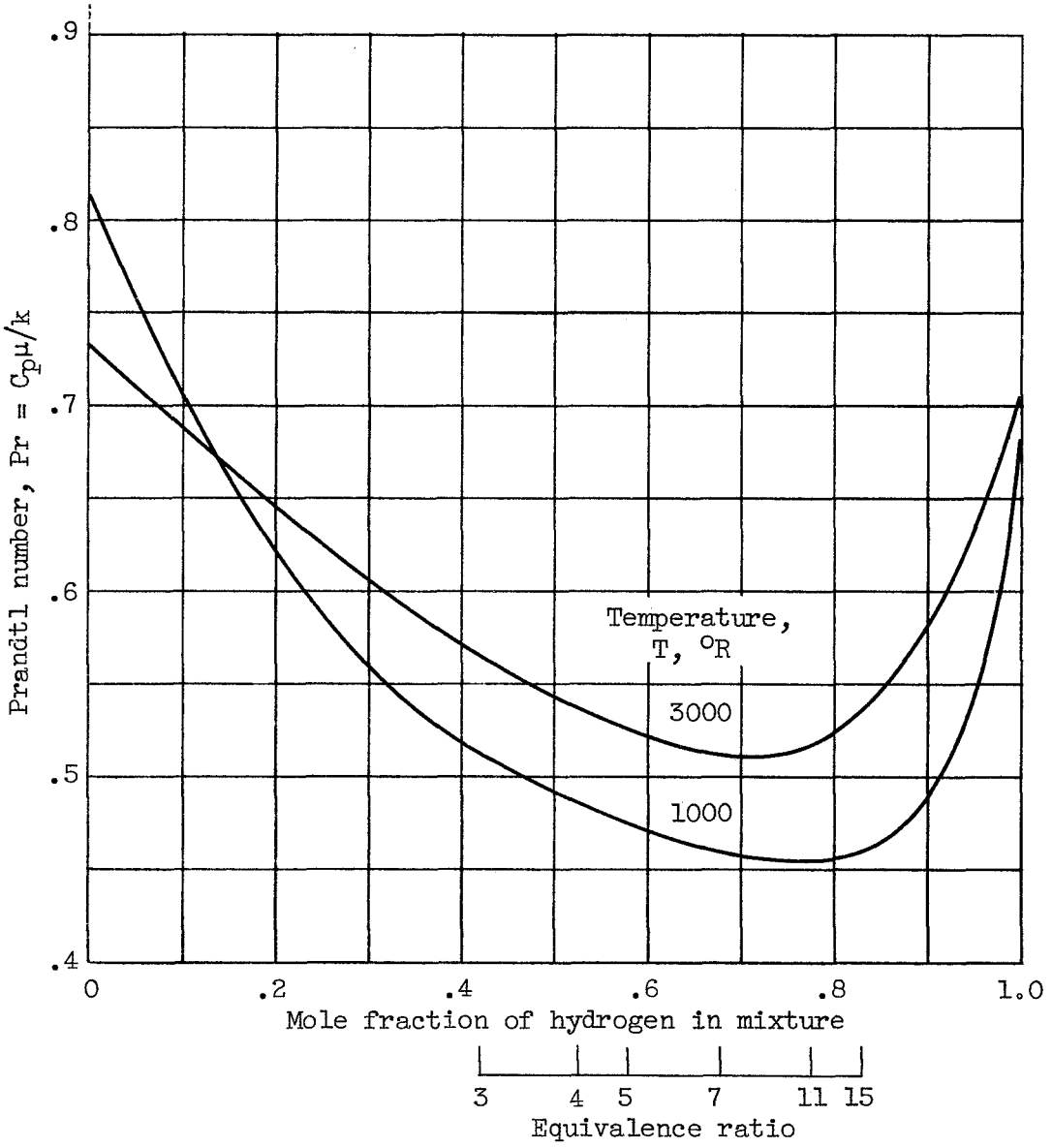

Figure 6. - Calculated Prandtl numbers of hydrogen-nitrogen-water vapor mixtures. Mole ratio of nitrogen/water = 3.77/2.0.

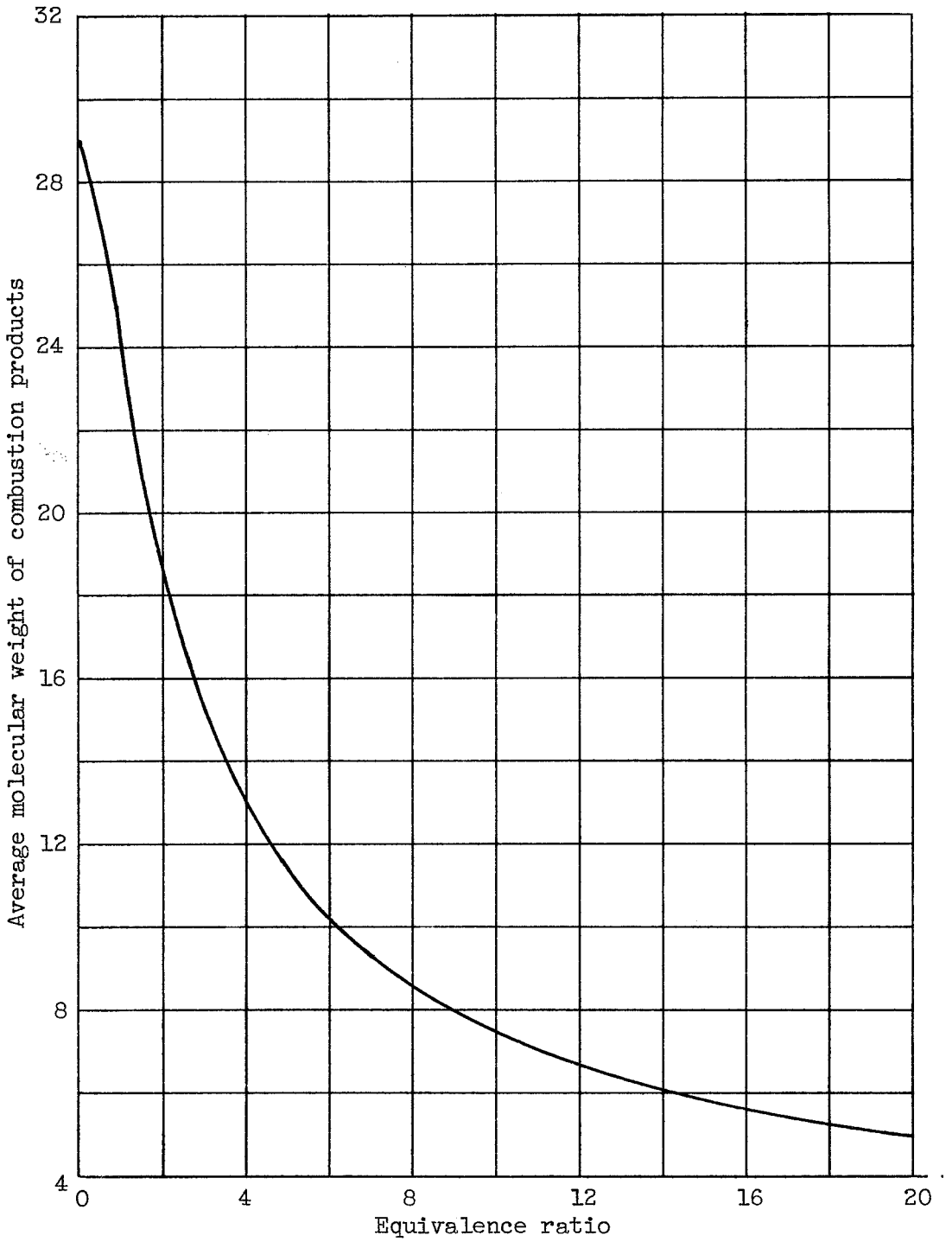

Figure 7. - Average molecular weight of combustion products of hydrogen-air mixtures. Products of complete oxidation with no dissociation.

4558

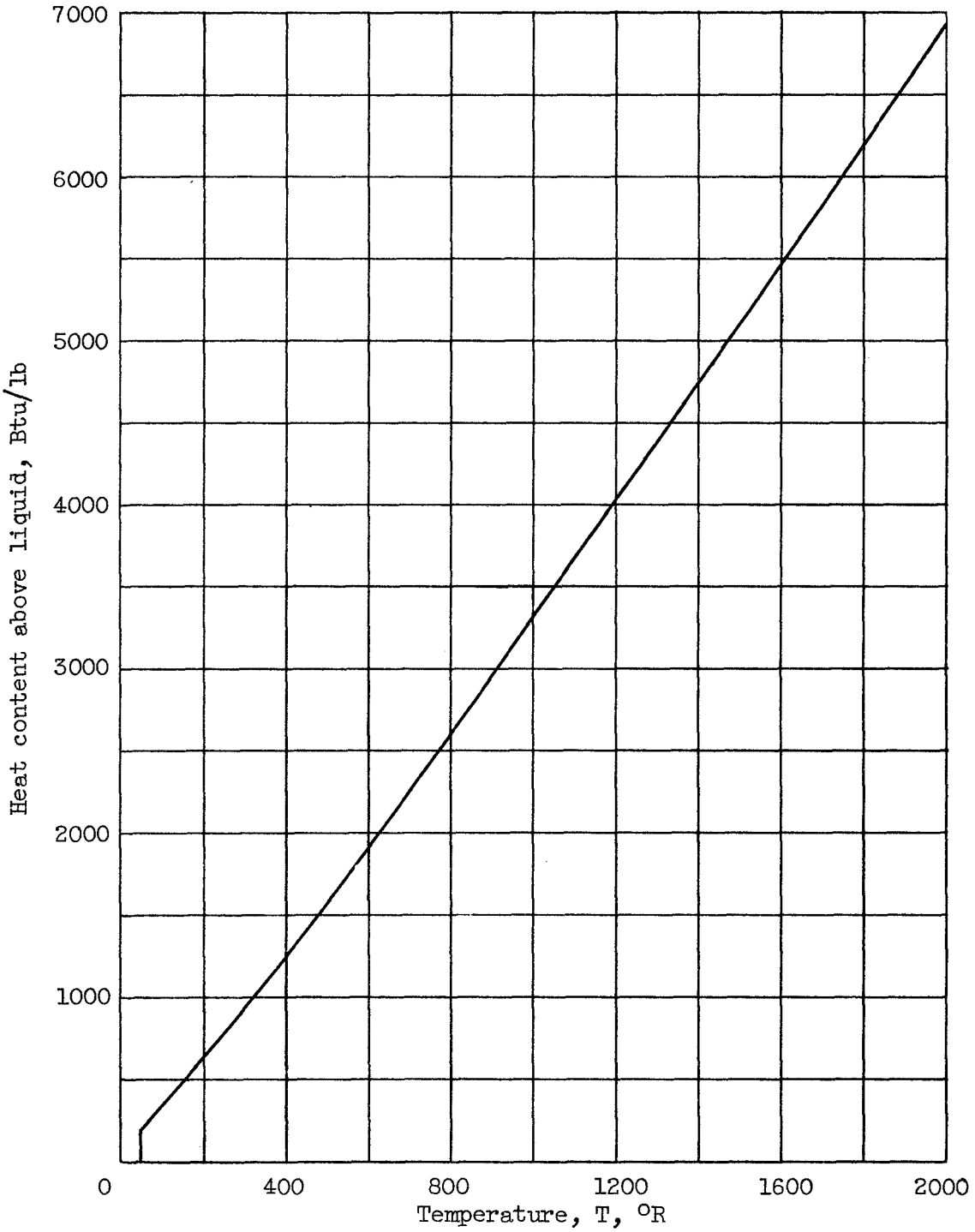

Figure 8. - Heat content of hydrogen above liquid at normal boiling point.

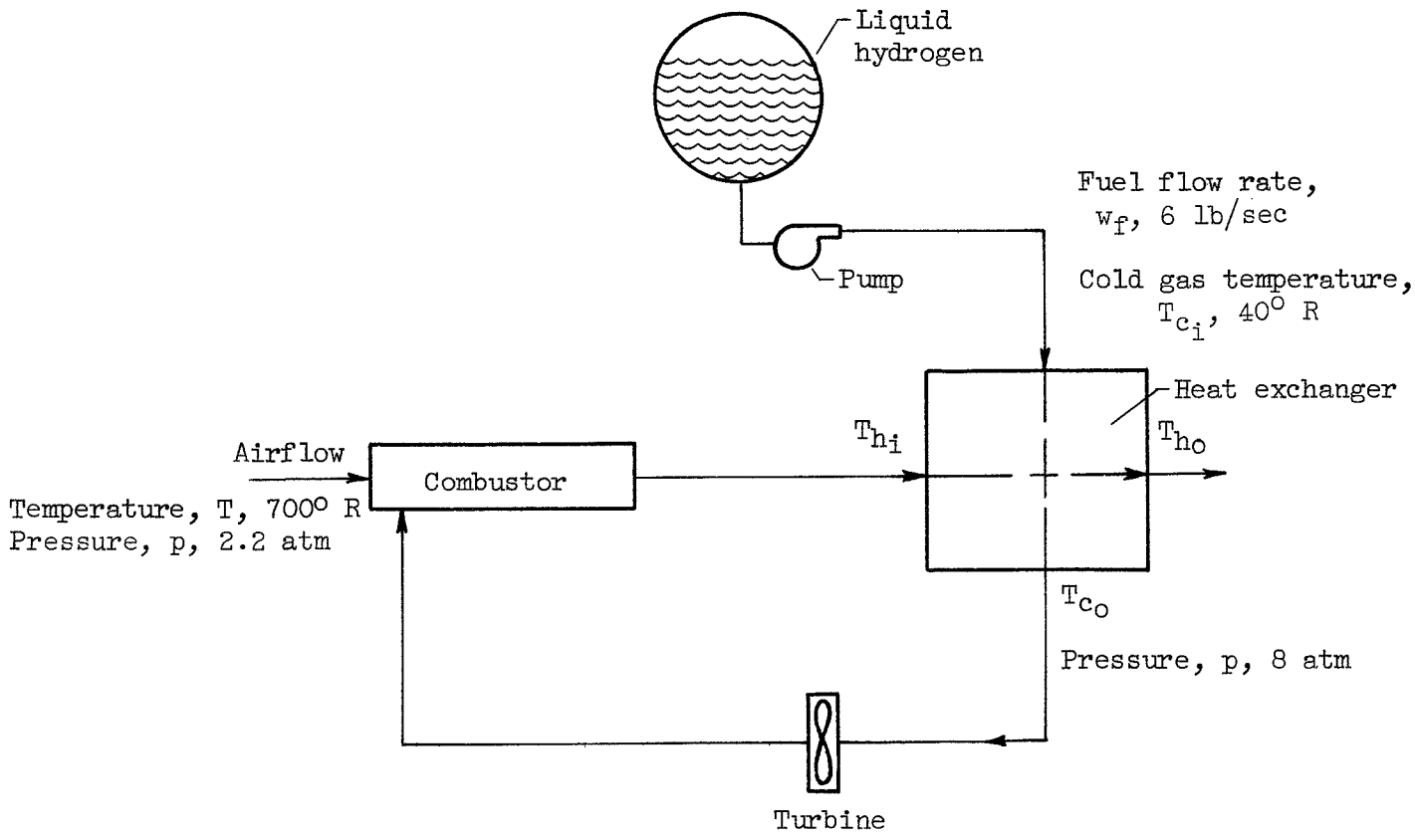

Figure 9. - Diagram showing relation of flow components under consideration.

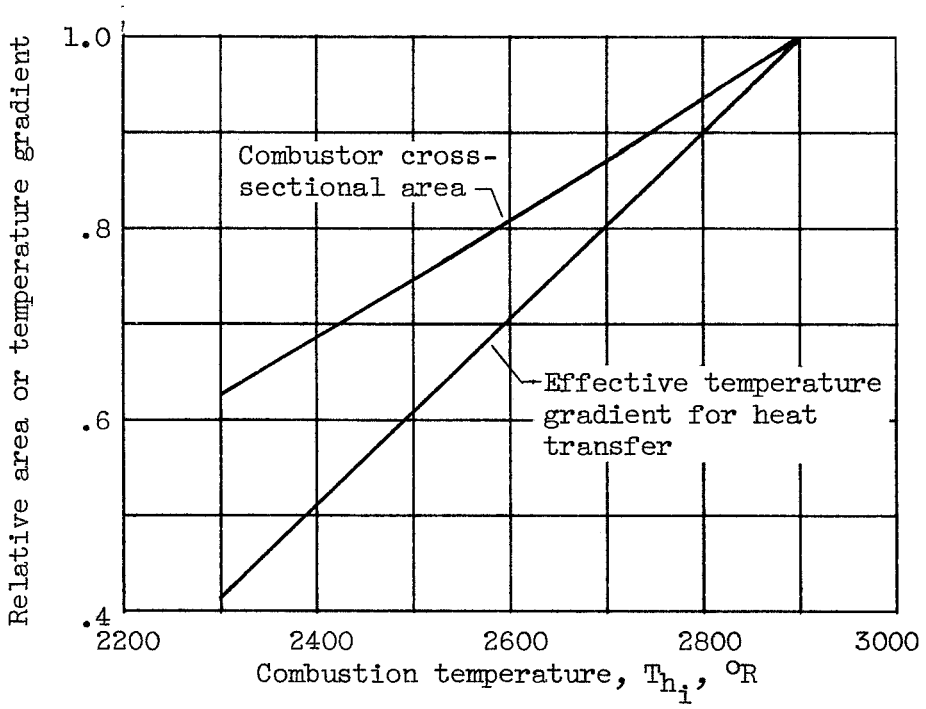

Figure 10. - Effect of combustion temperature on relative combustor area and on relative temperature gradient for heat transfer. Constant combustor-exit Mach number, 0.1.

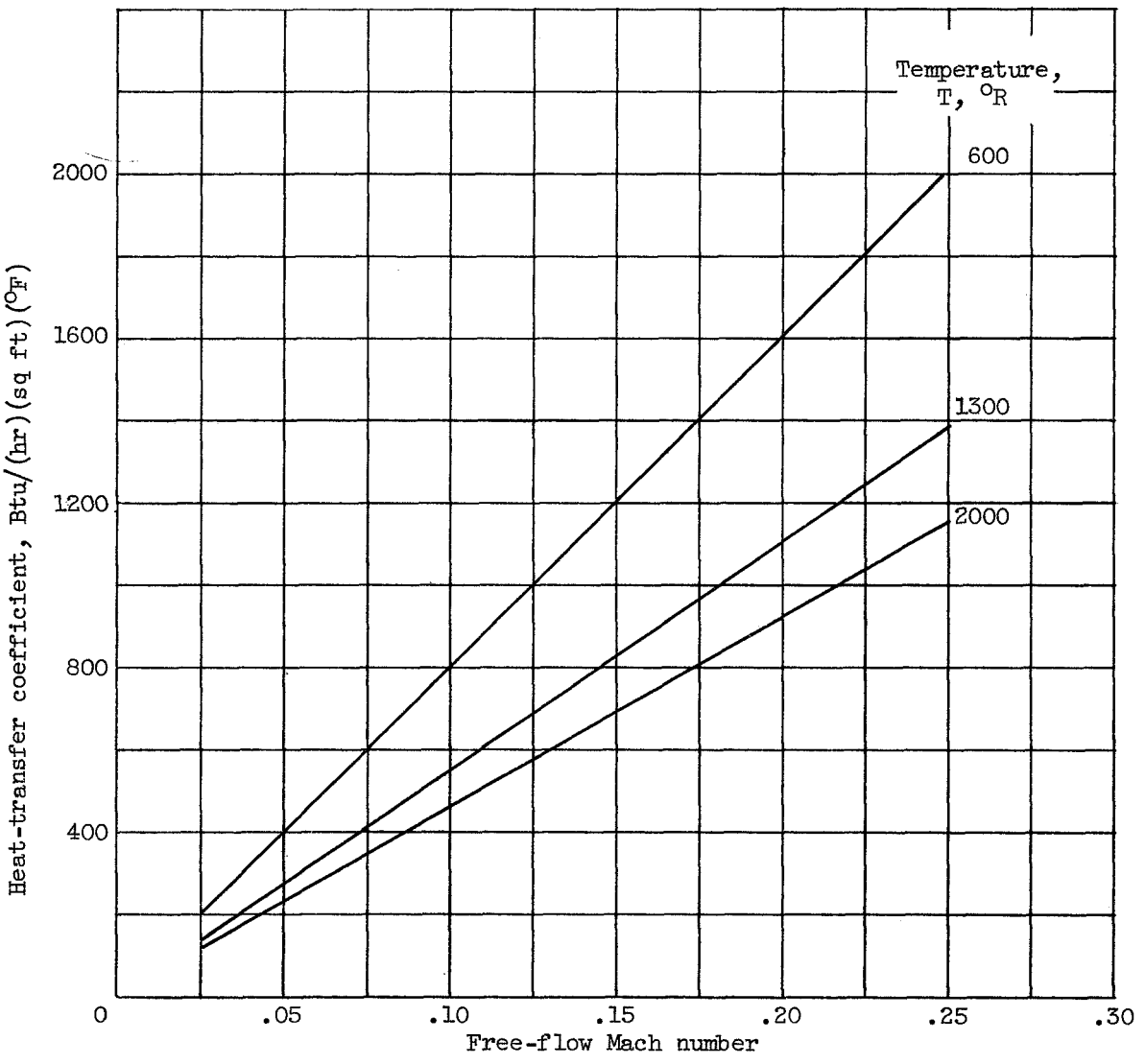

Figure 11. - Heat-transfer coefficient for hydrogen at 8-atmosphere pressure. $(St)(Pr)^{2/3} = 0.003$; $h = 3600 \frac{(St)(Pr)^{2/3}}{Pr}\left(pC_p\sqrt{\frac{\gamma gm}{R}}\right)\frac{M}{\sqrt{T}}$.

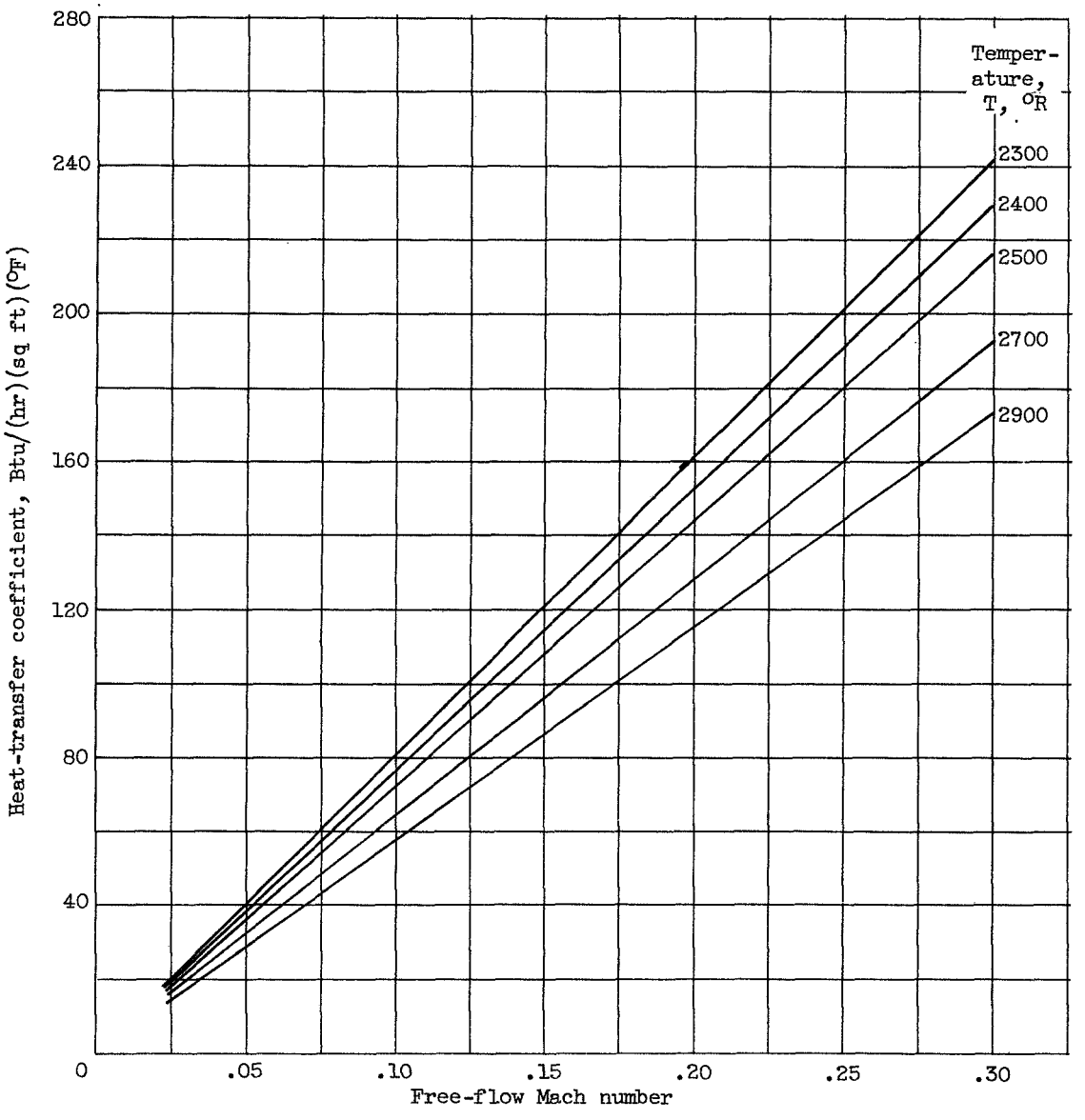

Figure 12. - Heat-transfer coefficient for hydrogen-rich mixture combustion products. Pressure, 2.2 atmospheres; $(St)(Pr)^{2/3} = 0.003$; $h = 3600 \frac{(St)(Pr)^{2/3}}{(Pr)^{2/3}} \left(pC_p \sqrt{\frac{\gamma g m}{R}} \right) \frac{M}{\sqrt{T}}$.

4558

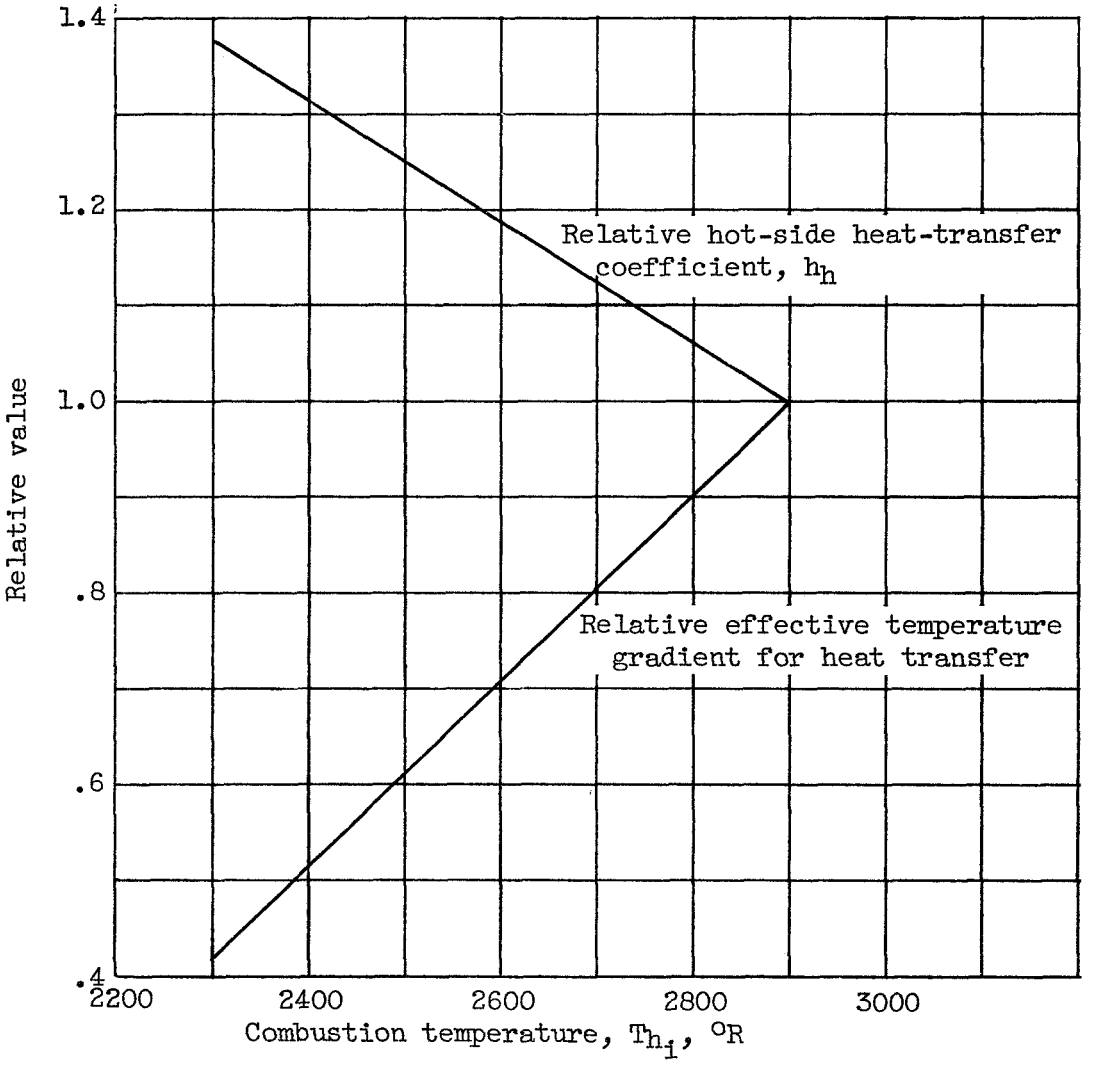

Figure 13. - Comparison of effect of combustion temperature on relative heat-transfer coefficient and relative effective temperature gradient for heat transfer.

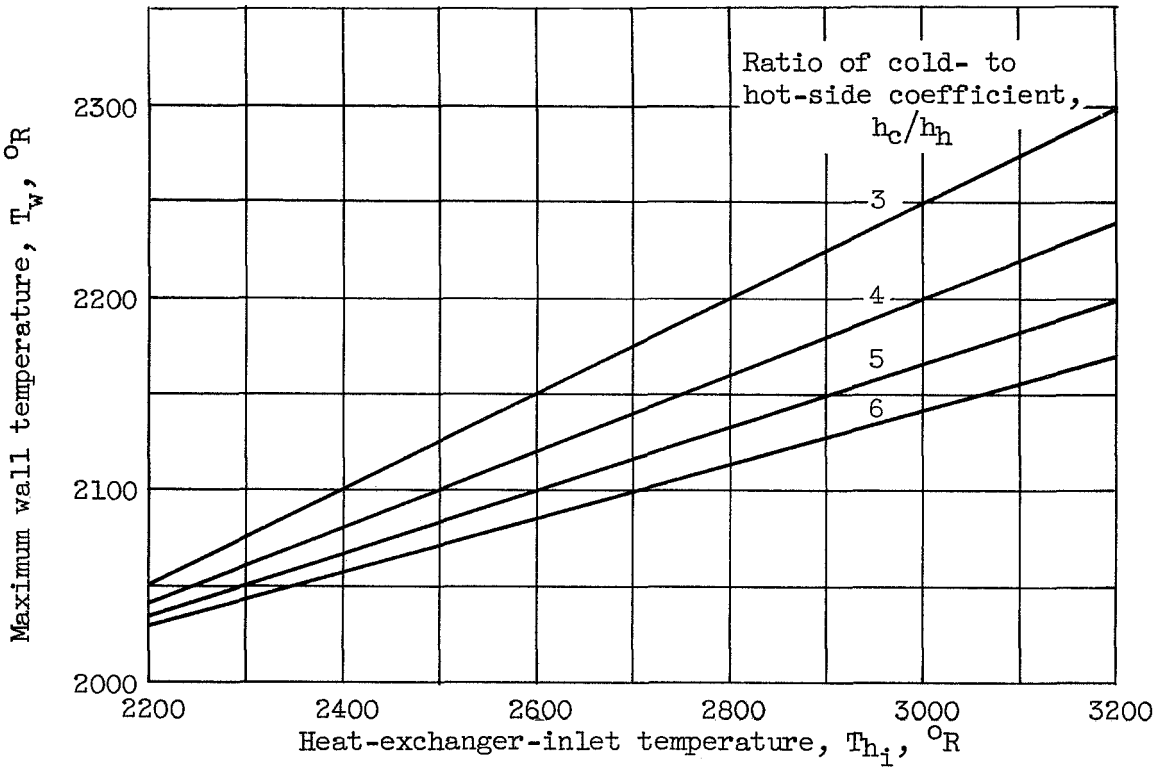

(a) Maximum wall temperature as determined from gas temperatures and relative heat-transfer coefficients. Hydrogen-outlet temperature, 2000° R.

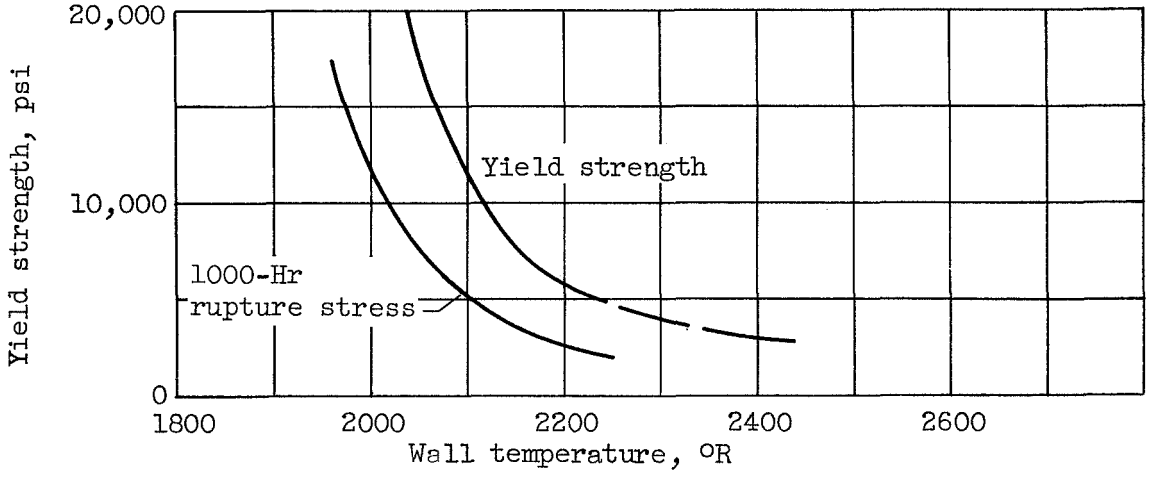

(b) Yield strength - temperature relation for a high-strength alloy, Inconel X (ref. 3).

Figure 14. - Parameters determining limiting wall temperature for stationary regenerator.

4558

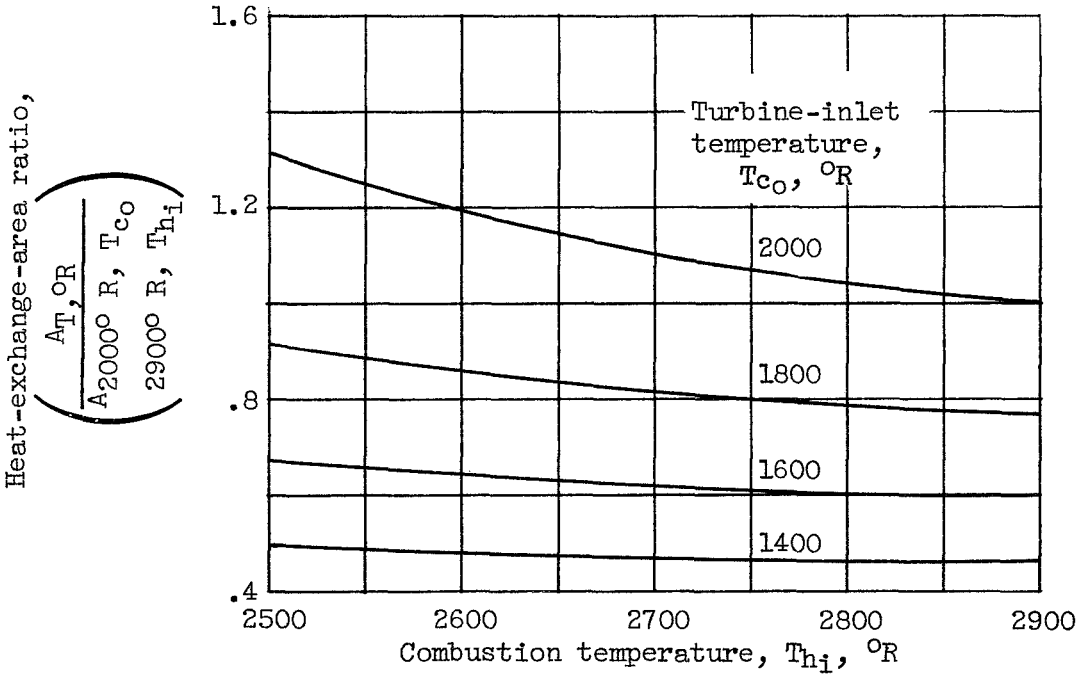

Figure 15. - Change in heat-transfer-area requirement with changing turbine-inlet temperature and combustion temperature. Stationary exchanger.

4558

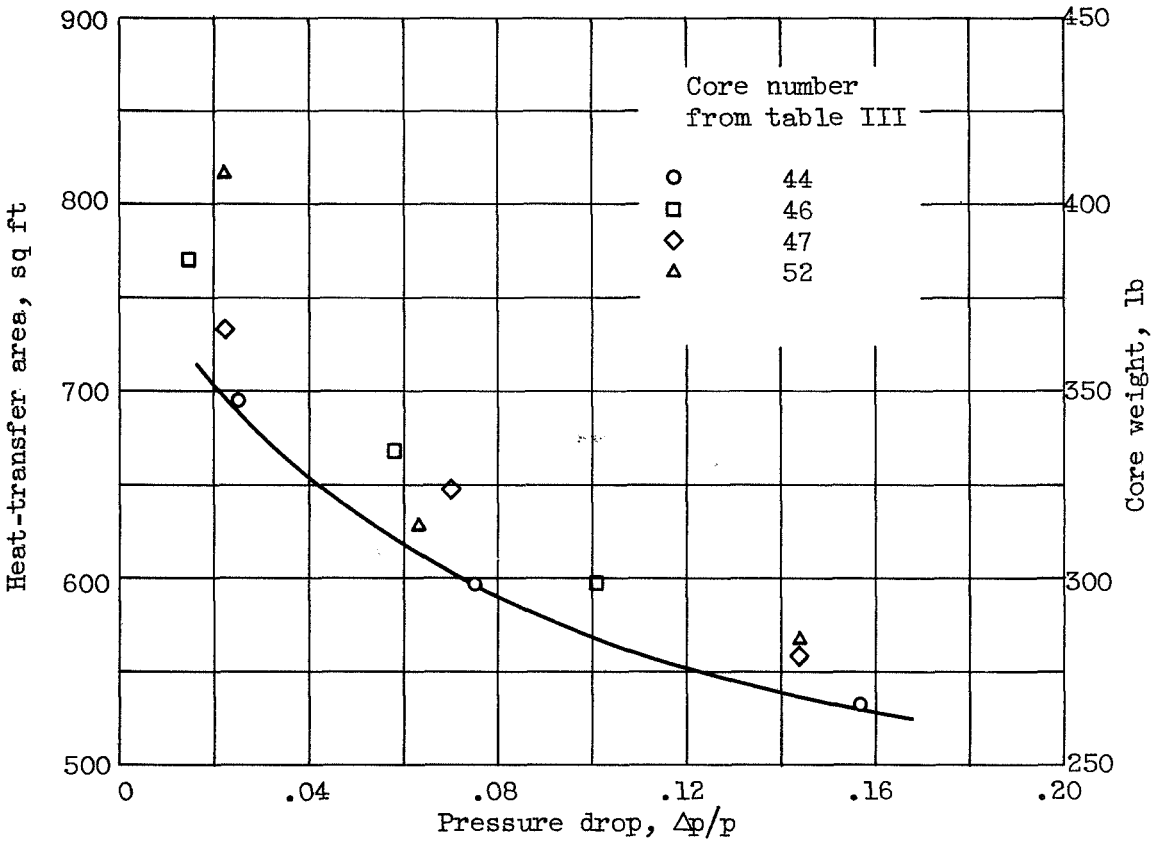

Figure 16. - Heat-exchanger-area - pressure-drop relations for several tube-shell core configurations.

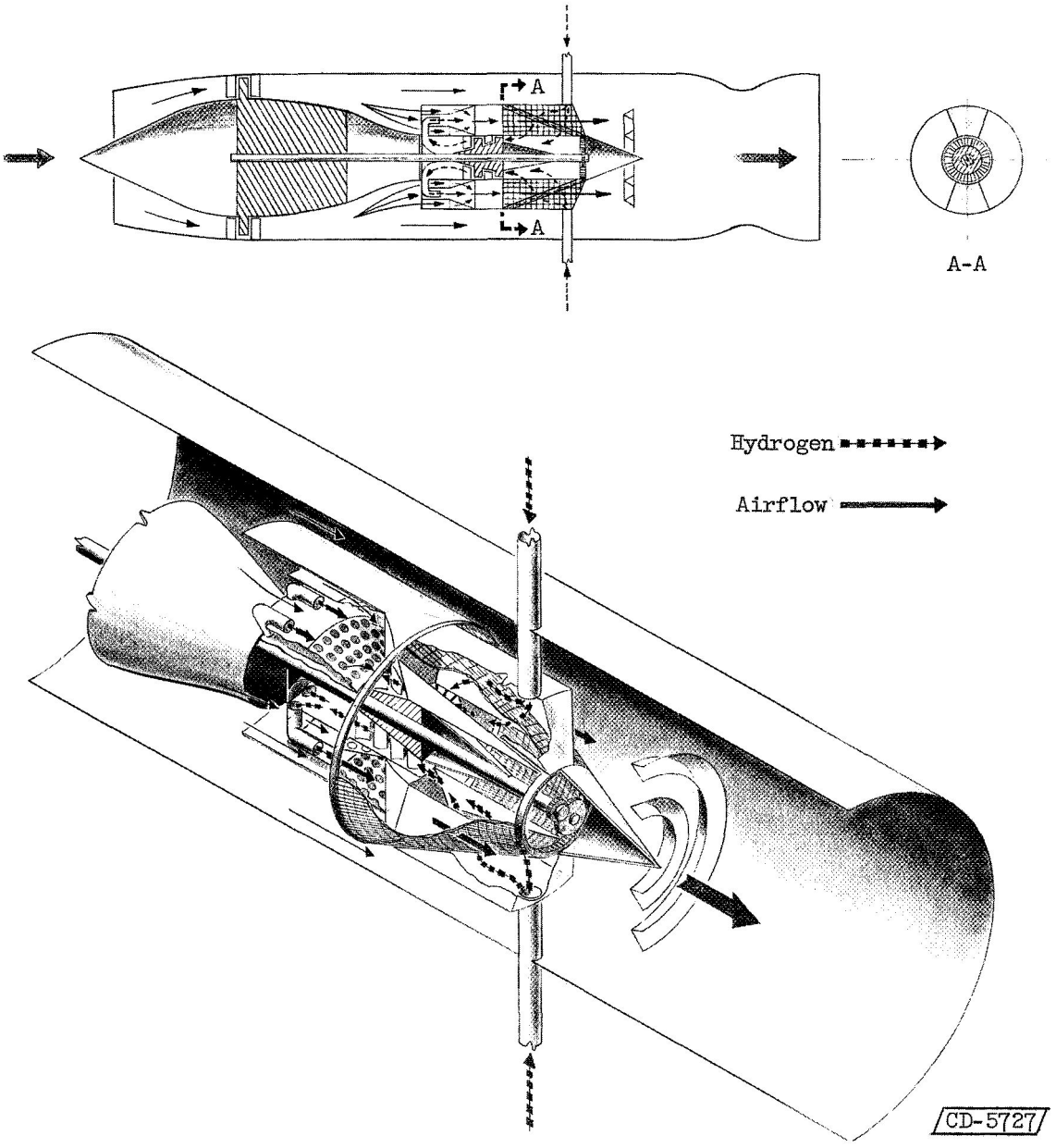

Figure 17. - Schematic diagram of Rex III cycle (ref. 1) engine with rotary heat exchanger.

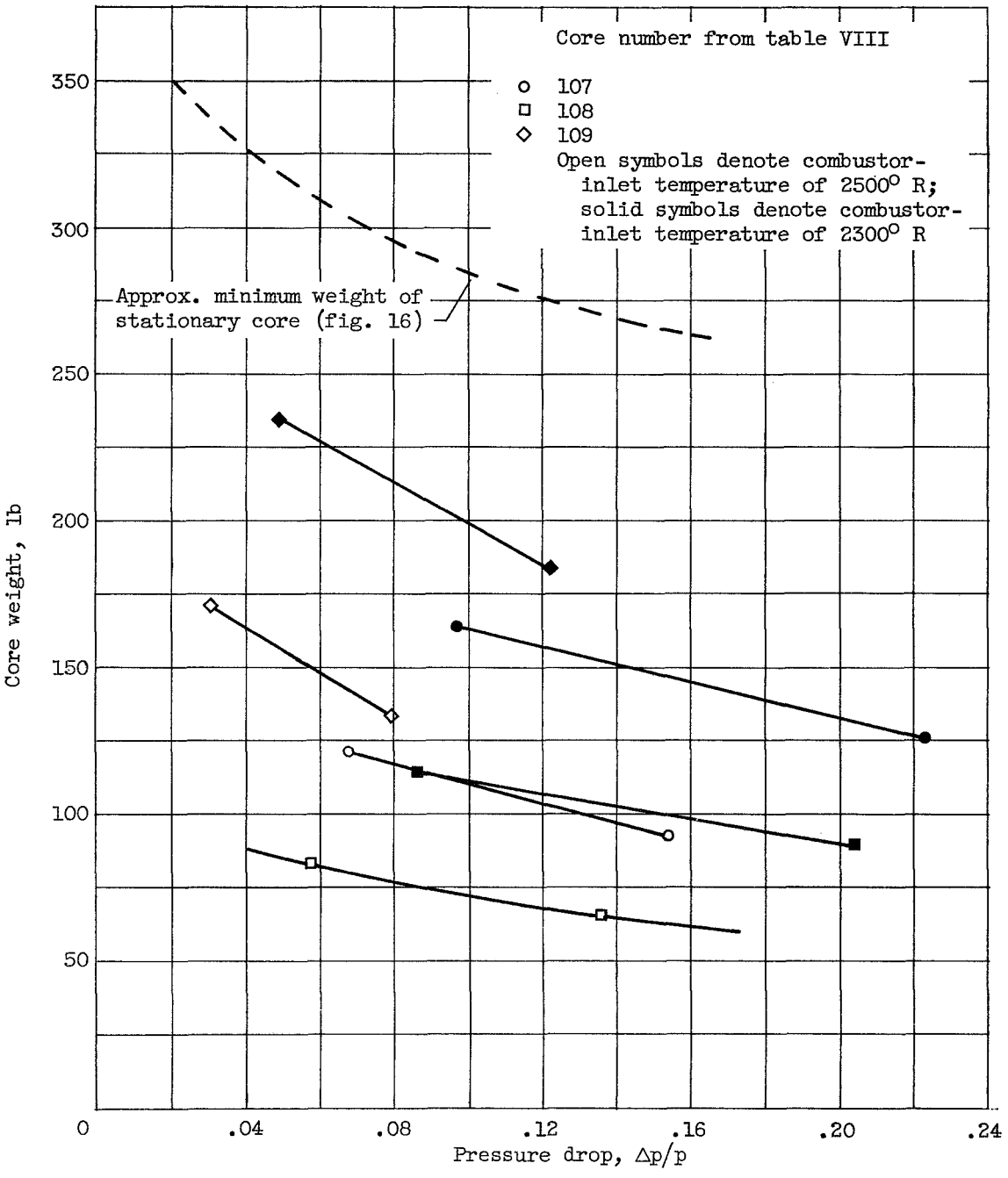

Figure 18. - Heat-exchanger-core weight - pressure-drop relation for several rotary heat exchangers.

4558

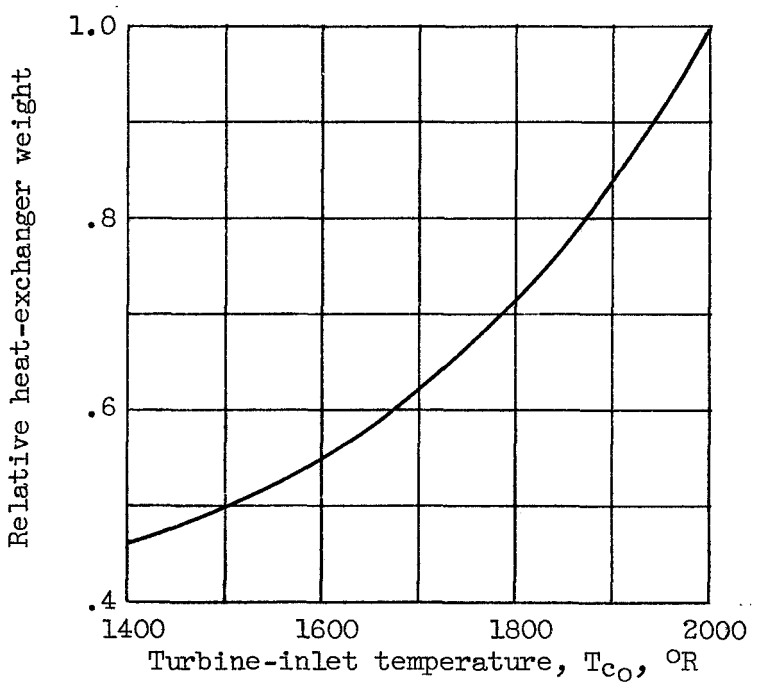

Figure 19. - Effect of varying turbine-inlet temperature on relative weight of rotary-heat-exchanger core.

CONFIDENTIAL

CONFIDENTIAL